RESERVOIR STUDIES OF NEW MULTILATERAL WELL ARCHITECTURE

A Thesis

by

MANOJ SARFARE

Submitted to the Office of Graduate Studies of
Texas A&M University
in partial fulfillment of the requirements for the degree of

MASTER OF SCIENCE

May 2004

Major Subject: Petroleum Engineering

RESERVOIR STUDIES OF NEW MULTILATERAL WELL ARCHITECTURE

A Thesis

by

MANOJ SARFARE

Submitted to Texas A&M University
in partial fulfillment of the requirements
for the degree of

MASTER OF SCIENCE

Approved as to style and content by:

Peter P. Valkó (Chair of Committee)	J. Bryan Maggard (Member)
Terry L. Kohutek (Member)	Stephen A. Holditch (Head of Department)

May 2004

Major Subject: Petroleum Engineering

ABSTRACT

Reservoir Studies of New Multilateral Well Architecture. (May 2004)

Manoj Sarfare, B.E., Maharashtra Institute of Technology, India

Chair of Advisory Committee: Dr. Peter P. Valkó

Hydrocarbon recovery from conventional reservoirs is decreasing and the need to produce oil cheaply from mature, marginal and unconventional reservoirs poses a big challenge to the industry today. Multilateral well technology can provide innovative solutions to these problems and prove to be the most likely tool to propel the industry in the next century. In this research we propose a new multilateral well architecture for more efficient and effective field drainage. We study the architecture from a reservoir engineering point of view and analyze the effect of various design parameters such as branch density and penetration extent of laterals on the performance of the proposed architecture for homogeneous reservoirs. We also analyze the performance in case of anisotropic reservoirs.

The numerical simulation results show that the multilateral wells usually help improve the overall cumulative production from a reservoir as compared to conventional wells. Also, they provide the added benefit of faster field drainage and present a more attractive return on investment. In this thesis we also present the results for a representative field case analysis. The rapidly changing Solution GOR contributed to making the oil viscous, which reduced the problem to optimize the mother bore location. In addition to these numerical studies we perform analytic studies to develop quick estimates of the theoretical limits of Productivity Index of the proposed architecture. We use known results from the literature to test their validity to estimate the upper and lower bounds on productivity. The results show that current tools to determine the lower limit is insufficient to predict performance.

DEDICATION

To my beloved mom, dad, and brother, who have always helped and supported me in all my endeavors.

ACKNOWLEDGEMENTS

I would like to take this opportunity to thank all those who helped and assisted me in completing this thesis. First and foremost, I extend my deepest gratitude to Dr. Peter Valkó, advisor and chair of my committee. His support, encouragement, and guidance have been invaluable in the successful completion of this thesis. He has been most patient and helpful all through my years as a graduate student at Texas A&M University.

I would like to thank Dr. Bryan Maggard for guiding me with my work. Also, I would like to thank Dr. Terry Kohutek for serving on my committee.

Friends have been a great source of advice during these years. Deepak, Ashish, Vivek, and Sandeep have provided a lot of tips towards writing the thesis and I sincerely thank them for the same. Harshal, Kartik, and DC, along with the others have helped make the long hours spent in the department quite enjoyable and pleasant. I have learnt new things all along the process and I thank everyone for their support and advice.

TABLE OF CONTENTS

Page

LIST OF FIGURES

LIST OF TABLES

TABLE Page

TABLE Page

CHAPTER I
INTRODUCTION – RESERVOIR APPLICATIONS OF MULTILATERAL WELL TECHNOLOGY

1.1 Introduction

Since their introduction in the early part of the last decade, multilateral well systems and their applications have developed rapidly[1]. They have been used in a myriad of operating conditions varying from mature fields to forming an integral part of completely new field development strategies. However under all the different operating arenas the aim is to produce hydrocarbons as quickly and efficiently as possible. In doing so the industry is faced by many challenges[2], some of which are:

1. complex geologic conditions such as compartmentalized or stacked reservoirs
2. difficult reservoir conditions such as viscous fluids or tight formations
3. hostile environments such as deep water or frontier development sites
4. efficient and effective reservoir management and development plans

Innovative solutions are necessary to tackle the problems and challenges facing the industry successfully. Multilateral well technology provides just such a solution. The technology has been successfully applied in all the above areas and shows a dramatic impact on the financial results of many, thus promising to be not just an evolutionary but also a revolutionary technology in the oil field.

1.2 Statement of Problem

Multilateral well has the potential for improvement in the productivity of a reservoir [3-5]. Over the last decade multilateral well technology[1] has been one of the most rapidly evolving and widely utilized production technology both for new as well as maturing reservoirs[2, 6-7]. Reservoir applications of multilateral wells have been discussed and the need to identify and quantify the reservoir benefits of this technology has

---

This thesis follows the style of *SPE Reservoir Evaluation and Engineering*.

received attention. With applications anticipated from the deepwater to the arctic, from heavy oil to gas condensate reservoirs and from small isolated lens[8] to giant field development – multilateral wells represent the leading edge in production technology.

Multilateral wells, used to develop fields in various locations[3], are classified into different forms or levels namely on the basis of the junction structure[8]. Hundreds of highly specialized multilateral wells have been successfully drilled and completed. The forum for Technical Advancement of Multilaterals (TAML) was created and a multilateral classification matrix was developed to foster better understanding of multilateral applications, capabilities and equipment. With the increasing maturity of reservoirs and the need to produce oil cheaper and quicker, multilateral well technology provides the industry with another tool to lower the cost of reserve development[1]. However this technology is still not widely accepted in the industry essentially due to the perceived high costs and the hesitation due to risks associated with implementing the technique.

In this thesis we propose an entirely new and advanced multilateral well architecture. It comprises a non-perforated horizontal mother bore with several laterals connected to it in the horizontal plane. The uniqueness of this architecture lies in the constructional and operational flexibility it affords for efficient reservoir drainage. We endeavor to further the present database of knowledge and understanding of multilateral wells with regards to reservoir engineering. To achieve this we study the parameters that affect the overall productivity of the new well architecture under various operational scenarios. While the final analysis with regards to feasibility of a technology depends greatly upon economic evaluation, it is beyond the scope of this study.

1.3 Multilateral Wells – An Overview

1.3.1 A Background of Multilateral Wells

It is acknowledged that the father of multilateral (ML) wells is Alexander Grigoryan[9]. In 1949, he developed an interest in the theoretical work of American scientist L. Yuren, who maintained that increased production could be achieved by increasing the diameter of the borehole in the productive zone of the formation.

Grigoryan took this theory a step further and proposed branching the borehole in the productive zone to increase surface exposure.

He put this theory into practice in the former U.S.S.R. field called Bashkiria (now known as Bashkortostan). His target in this field was an interval in the range of 10 to 60 m (33 to 197 ft) in thickness. He drilled to a depth of 575 m above the pay zone and then drilled nine branches from the open borehole. Compared with the other wells in the field this well was 1.5 times more expensive, but penetrated 5.5 times the pay thickness and produced 17 times more oil each day. This unprecedented success inspired the Soviets to drill an additional 110 ML wells.

1.3.2 Present State of Multilateral Wells

Inspite of the success of the early ML wells, they have not yet evolved to the point of being the industry norm today. Like horizontal wells, ML well application is justified through their economic viability. Defined as a single well with one or more branches emanating from the main borehole, their aim is to improve production while saving time and money. The complexity of ML wells ranges from simple to extremely complex structures. According to the TAML classification ML wells are classified into 6 levels, shown in Figure 1.1, though they can be simply classified into two groups as:

- Wells that require pressure integrity at the junction
- Wells that do not require pressure integrity at the junction.

The characteristics of the various levels are[10]:

Level 1 - There is an openhole junction between the mainbore and the lateral.

Level 2 - The junction is constructed to be openhole extending from a cased and cemented mainbore.

Level 3 - This is a slight modification of the Level 2 junction in that the lateral borehole is drilled from a cased and cemented mainbore. However in addition a slotted liner or screen is placed in the lateral and tied back to the mainbore through a hanger device.

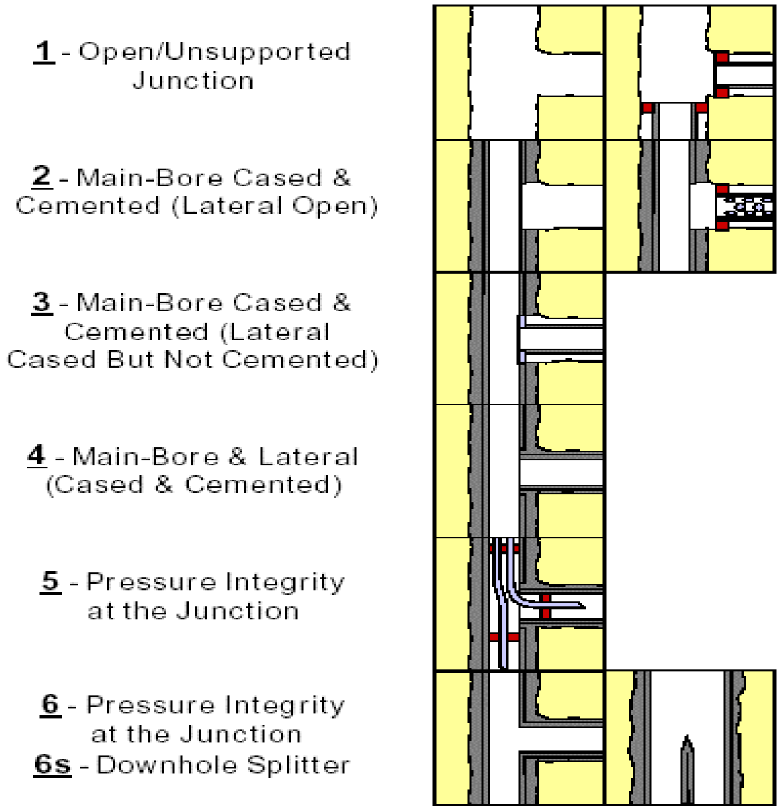

Figure 1.1 – TAML classification of ML wells[10]

Level 4 - The lateral borehole extends from a cased and cemented mainbore. The junction is constructed such that a lateral liner is cemented back to the mainbore.

Level 5 - This junction is described as a pressure seal across the junction established by the completion equipment. Packers and other seals may be used along with dual tubing strings to obtain a three-way pressure seal.

Level 6 - This junction provides for a pressure seal established by the casing itself. It is typically employed at the bottom of a casing string. After the casing and junction are cemented into place the laterals are drilled and tied back to the junction with some cemented lateral liner and hanger assembly.

ML wells with TAML junction levels 1 through 4 have been applied extensively in the new and maturing reservoirs of all sectors of the North Sea[3]. A Level 4 ML well has been successfully used in the Tern field in the North Sea. The Troll Olje field also in the North Sea is another example where ML technology was found more appropriate than conventional technologies[11]. Multilaterals have provided a means to optimize slot usage, commercially develop lower-quality reserves in the Brent sequence and when applied with complementary technologies of underbalanced drilling and intelligent well completions help optimize field development

The economic benefits of ML wells compared to horizontal wells in water-drive reservoirs in varying permeability fields has been investigated and found to have a better net present value[12]. A level 6 junction was used to simulate the performance of ML wells. Also when OOIP is lower the performance of a multilateral well is better than a horizontal well. The use of ML technology improved the recovery factor by water flooding in a mature oil field in Venezuela. The recovery factor, economic viability and lowest operational activity were achieved for a ML development scheme compared to the vertical well concept[13]. Level 4 ML technology in conjunction with intelligent systems helped improve the recovery at Wytch Farm, UK[14]. This scheme not only helped to recover the marginal reserves but also added new production at reduced risk. The Mukhaizna field, south Oman contains 14-16° API oil in unconsolidated sand[15]. The possibility of early water breakthrough posed further technical difficulties in producing the heavy crude. However the use of dual lateral wells helped make the project a very attractive investment opportunity.

Also studies have been performed to predict the performance of multilateral wells. Larsen[16] computes the productivity indices or skin values for arbitrary well configurations in homogeneous reservoirs of constant thickness. Symmetry of the reservoirs is an important requirement in this computational technique. Other models to predict ML well performance assume the well to be divided into various segments and computations are performed on each of these segments. Salas[17] models the Well Index factor for ML wells by accounting for competition effects of inflow performance and interference effects of commingled production of branched wells. A transient model[18] for ML wells is developed that can be applied in commingled reservoirs. The model accounts for crossflow between layers.

The ML wells applications mentioned above essentially address the various challenges facing the industry mentioned earlier. The history of the last decade of ML wells has helped establish the business driver for ML technology[19]. However inspite the successful application of ML technology in the oilfield the industry is hesitant to accept this technology in a big way. This inertia arises from the fact that the behavior of ML wells is not completely understood and the difficulty to evaluate the potential benefits of ML technology. The lack of willingness to adapt to it can be ascribed to the following reasons:

1. Reliability

   Despite the high technical and economic success of ML wells they are still viewed to be associated with a great amount of risk. This perception exists though the industry wide statistics suggest otherwise.

2. Value

   Even the operators most experienced with ML technology are sometimes hard pressed in identifying and quantifying the true value and return on investment of these wells. This is partly due to the inability to perform effective modeling and prediction of well performance and lateral contributions.

1.3.3 The Future

The future of ML wells is in harder-to-drill formations where the reservoirs require selective completions, selective isolations and stimulation operations. They could also be used in exploration wells, to mitigate geologic risks and navigate heterogeneous reservoirs[1]. The future of the oil and gas business[20] lies in unconventional reservoirs like tight-gas sands, coalbed methane, heavy oil and gas shales. To be able to produce these resources economically improved technology will be in greater demand. Many current technologies like hydraulic fracturing, steam injection will definitely be applicable along with improved reservoir characterization methods to reduce risk. But in addition to this the ability to produce the resources to the surface will need the development of multibranched well bores. Greater recoveries coupled with economic attractiveness will definitely help improve the confidence of operators in this nascent technology.

CHAPTER II
NEW MULTILATERAL WELL ARCHITECTURE

2.1 Description of the New Multi-lateral Well Architecture

Consider a reservoir or a part of it that has a rectangular cross-section along its depth. The new multilateral well architecture [21] consists of a horizontal well penetrating almost the entire length of the reservoir along with branches from the horizontal in the lateral direction. A vertical well is connected to one end, heel, of the horizontal well and it acts as the point of vertical lift. The other end of the horizontal is the toe so that the flow in the horizontal is from toe to heel. Hence there is only one vertical conduit acting as the production string. The main horizontal section (collector well or mother bore) is not perforated but contains several pre-prepared junctions. The diameter and completion type of the vertical and the main horizontal sections are such that they maximize the pipe flow capacity. The horizontal wellbore and the surrounding reservoir are completely isolated. Once cemented the vertical and horizontal sections are not readily accessible with well intervention tools. The junction equipment is placed during the drilling of the main horizontal well and it is cemented together with the main horizontal section. The pressure and structural integrity of these junctions is a critical requirement. However unlike traditional multilateral wells this integrity is not compromised by additional requirements such as potential capability of future well intervention, formation damage control during drilling or ability to accept tools in a later phase.

Once the main horizontal well bore is drilled the other laterals are drilled from one or more locations on the surface. The laterals are drilled in a direction perpendicular to the main horizontal well. The feeder lateral is connected to the main mother bore at the pre-prepared junction points. They are completed in a number of ways while focusing on maximizing the inflow potential without compromising it by additional requirements. For example relatively slim holes are acceptable as they are less capital intensive, not prepared to accept tools at a later stage and might be completed open-hole or frac-packed and hence disposable. Also the time schedule of feeder lateral drilling is very flexible and can change depending upon further information collected from the field and on market requirements.

The proposed architecture can be better understood from the Figure 2.1 given below. As shown in the figure, 25b is the main horizontal well with intersection points represented as 22 is placed in the casing. Well 226 is drilled with multiple feeder laterals

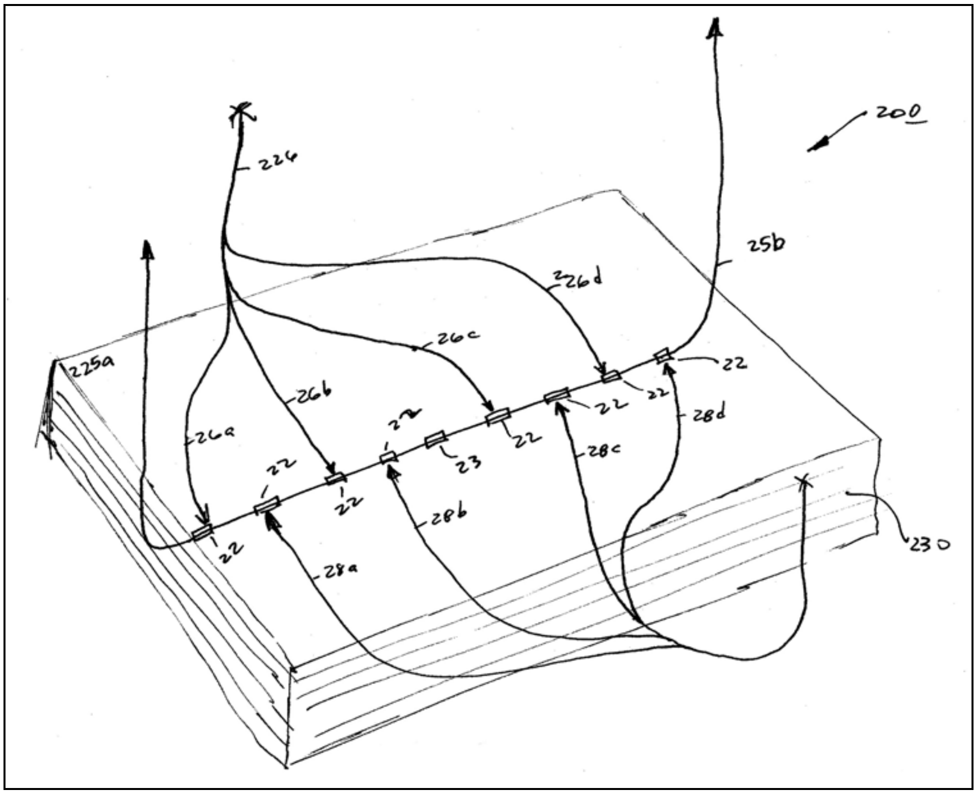

Figure 2.1- New multilateral well architecture

26a, b, c, d all connecting into the parent well. The casing of the feeder well intersects the casing of the parent well and is mechanically connected and sealed at the intersection points. Production flows from the toe of the feeder well into the mother bore to be lifted to the surface. A plug is used to prevent cross flow or pressure transition exposures at the junctions between the feeders (26) and the access well (226). In the well network so formed the feeders do not have to carry all the production of the field and so can be smaller in diameter. The mother bore is a larger well bore so that it can handle the large flow rates.

The proposed architecture is radically new as the collector well is not used for lateral drilling or any well intervention in the laterals. Thus the continuity of production is not jeopardized on account of any event in the laterals. In fact there is a separation of two functions: one is to collect hydrocarbons from the reservoir as performed by the laterals and the other is to conduct the hydrocarbons to the point of vertical lift and ultimately to the surface.

2.2 Advantages of ML Wells

The various advantages of multilateral wells can be summarized as follows:

1. Reduction in well costs. This is due to the need to use fewer top-side and near surface equipment for a single multilateral well as compared to a group of conventional wells.
2. Mechanically sealed junctions with full casing integrity eliminate one of the main failure point as compared to other multilateral designs
3. Improves sweep efficiency by delaying gas or water breakthrough.
4. Facilitates better drainage of heterogeneous reservoir systems.
5. Enhances production for difficult fluids.
6. Reduction of environmental footprint.
7. Increases the reservoir exposure.
8. Better connects the natural reservoir permeability
9. Greater exposure accelerates the production rate.
10. Accelerated production also allows for early production of secondary or marginal reserves.
11. Reduced overall project costs improving the rate of return.

2.3 Multilateral Well Model

From a reservoir engineering point of view it is difficult to quantify various advantages of the proposed multilateral well architecture. However it is possible to investigate quantitatively [21] the productivity of the new well architecture through numerical simulations. To simulate the proposed architecture the well bore structure is modeled as a main horizontal wellbore fed by many parallel laterals. This structure is shown in Figure 2.2. The reservoir essentially contains a vertical well bore that conducts the fluids to the surface. From this vertical, a main horizontal section called mother bore is drilled to penetrate the entire length of the reservoir in the direction of the largest horizontal dimension. Now feeder laterals are connected to the mother bore at the pre-prepared junction points. One lateral is drilled on either side of the mother bore so that they form a network of alternately placed laterals. The laterals are perpendicular to the mother bore and are in the direction of the smallest horizontal dimension.

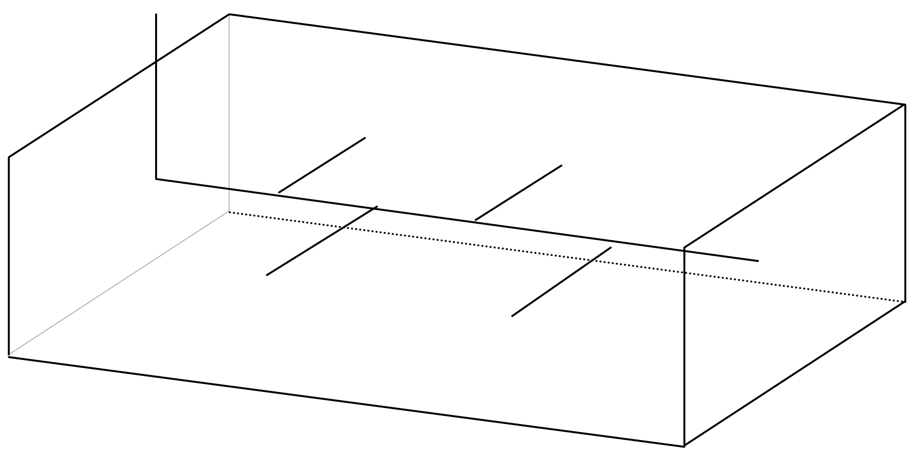

Figure 2.2 – Multilateral well model used for numerical simulations

As shown in the figure depending upon the branch density, we can have all the laterals drilled or any subset of it. In addition we can drill the laterals reaching the outer boundary of the drainage volume (100% penetration) or we can assume a smaller percentage of penetration. In the model the mother bore is not perforated and the feeder laterals are perforated (or completed open hole) providing communication with the reservoir. Formation damage in the vicinity of the laterals is neglected. This is because the feeder laterals are drilled and completed with the requirement of minimum formation damage made possible by lack of necessity to compromise for well integrity, larger hole diameter, preparing for additional drilling activity, preparing for sophisticated completion equipment. Also frictional pressure losses in the main horizontal section are neglected due to its large diameter.

2.4 Methodology and Procedure

The first task in evaluating the performance of the suggested well architecture would be to identify the types of reservoir applications for which the technology may be used. From this point of view various parameters affecting the performance of multilateral wells must be identified and analyzed. In this work we focus on the reservoir engineering aspects, investigating such issues as the effect of branch density (number of laterals) and the penetration of laterals (with respect to the lateral dimensions of the reservoir). The main issue is the overall productivity of the well architecture as a complex drainage tool.

The primary tool to do such investigations is reservoir simulation. However it is also important to put the results into perspective, partly by comparing them to more conventional drainage systems and partly by establishing theoretical limits. Such a methodology ensures that no false anticipations are generated and a realistic evaluation can be performed.

The obvious reservoir engineering approach to do this job is to establish a “base case” and perform parametric studies. We perform simulations using Eclipse – one of the most widely used reservoir simulators in the industry. The multilateral well model discussed above forms the basis of these parametric studies. The lateral configurations are changed as per the investigative needs.

Firstly the performance is investigated in a homogeneous reservoir model. In this model, we build rectangular reservoir with the architecture proposed above. In all the models we can have up to 60 laterals producing into the mother bore. Branch density and penetration of laterals are the two basic parameters that most affect overall productivity. Assume that a multilateral well must be designed to drain the net pay for a given reservoir. The very first question that arises is: what should be the number of feeder laterals drilled? The next issue is: how far should these laterals penetrate into the bulk of the reservoir. While this decision will depend upon the cost of drilling and completion, various additional factors such as hydrocarbons in place, reservoir structure, driving mechanism and others will influence the final answer. Hence our strategy is to evaluate the simplest assumptions through this preliminary analysis and consider the additional details with particular reservoirs. Along with the homogeneous case we try to incorporate heterogeneity in the model by using anisotropic reservoirs.

Secondly, representative cases will be set up for field data. Reservoir and fluid data are used to prepare models wherein a part of the actual field is represented as the rectangular reservoir we use in the preliminary analysis. The performance of the multilateral well architecture will be compared with that of conventional vertical wells.

2.5 Technical Indicator

Cumulative production is one of the most important quantities considered while making a decision about the feasibility of any field development theme. In addition to cumulative production (in a certain amount of time) one should consider the actual distribution of production in time. However both cumulative production and its distribution in time both have only a limited information value, if we cannot compare it to some ideal drainage structure or an existing well architecture.

The reservoir engineering concept of Productivity Index [22] (PI) is a quantity which helps to put the various results into perspective. While traditionally this concept is used mostly for a single well, its generalization is a valuable tool to evaluate complex well architectures. Also it can be un-dimensionalized in a format that is representative not only for a given reservoir-fluid system, but for a whole family of them.

Productivity index essentially describes a linear relationship between the production rate and the driving force. For practical and theoretical purposes we select the driving force as the drawdown pressure. The drawdown pressure is defined as the average pressure in the reservoir minus the average pressure along the sink surface (i.e. the wellbore pressure). The Productivity Index, denoted by J is given by,

$$J = \frac{q}{p_{res} - p_{wf}} \quad \text{.......... (2.1)}$$

where p_{res} is the average volumetric pressure in the reservoir and p_{wf} is the wellbore flowing pressure.

The value calculated from equation 1 in general is not constant in the transient flow regime as J decreases with time. In the stabilized flow regime the PI is constant. There are three main stabilized flow regimes:

Steady-state

The boundary at the top and bottom are no flow. A constant pressure is assumed at the outer boundary of the reservoir in the lateral directions. In addition, p_{wf} or the production rate is kept constant. The steady-state is characterized by a non-changing pressure distribution in the reservoir.

Pseudo-steady state

Again the boundary condition at the top and bottom are no flow. At the outer boundary of the reservoir in the lateral directions we assume the same conditions: no flow across the boundaries. Such an idealization is often called a volumetric reservoir. In addition we keep constant total production rate. The pseudo-steady state represents the long-time limiting behavior of the reservoir and is characterized by a constant change in pressure with time everywhere in the reservoir. This implies that the shape of pressure distribution in the reservoir is preserved during production though the reservoir is being depleted at a uniform depletion rate. However such a regime cannot be maintained forever, because the reservoir is depleted at a constant rate and hence the wellbore pressure is also decreasing with a constant rate and will ultimately reach a physical limit of zero pressure.

Boundary-dominated state

Once more the top and bottom boundaries are at no flow condition. At the outer boundary of the reservoir in the lateral directions we assume no flow condition with a constant wellbore pressure. The boundary-dominated state is the long-time limiting behavior of the system and is characterized by a completely different pressure distribution than the pseudo-steady state pressure distribution. Under boundary-dominated flow the rate of depletion depends both upon the location as well as the time, but the rate of change of depletion rate is a function of location only. At any particular instant the depletion rate is such a function of location that the further the location from the nearest wellbore larger is the depletion rate at that location. Such a flow regime exhibits a continuously decreasing production rate and a similarly decreasing drawdown.

Though Productivity Index is a valuable technical indicator only factors like oil in place and profit analysis will essentially determine the optimum Productivity Index to be used. In practice, however it is observed that the increase in Productivity Index requires investment but the relation between PI and cost increase is very stochastic in nature.

CHAPTER III
ESTIMATION OF THEORETICAL UPPER AND LOWER LIMITS

3.1 Motivation

The need to provide a theoretical framework for the simulation results obtained in the later part of the research is a major driving force in performing the analytical work presented in this chapter. A firm theoretical basis is necessary to put numerical results into perspective and be confident of the results obtained in a new study. The architecture studied in this thesis is unique and hitherto uninvestigated in the literature. Also the currently available models to evaluate the productivity of a single ML well comprises variables and effects that are not applicable in the cases we analyze and hence are not suited to predict the performance accurately. Some of these variables are those of friction effect in the flowline and crossflow between layers.

As mentioned earlier the PI is a very effective tool in analyzing well performance and comparing different reservoir flow systems. Hence the objective of the material presented in this chapter is to develop back of the envelope methods to obtain theoretical limits of productivity index attainable by the advanced well architecture design.

3.2 Methodology

We aim to obtain a theoretical upper and lower limit for the productivity of the proposed well architecture for some particular cases and to do so we use results available in the literature to model the fluid flow in a ML well.

The concept of infinite fracture conductivity[23] is used to establish the maximum PI obtainable by the ML well architecture. The flow into the laterals penetrating the smaller horizontal dimension of a reservoir is linear. This is similar to the linear flow into an infinite conductivity fracture, which extends from the well bore to the lateral reservoir boundaries in the vertical plane. An infinite conductivity fracture is characterized by negligible pressure drop in the flow direction and hence represents the greatest throughput of fluids as per the definition of PI. The flow is both linear as well as perpendicular to the fracture and the laterals. In order to model the ML well as an infinite conductivity fracture we assume infinite lateral branch density in the horizontal plane.

Since we neglect the frictional pressure drop in the laterals the fluids will be conveyed to the mother bore instantly without any need to expend fluid energy to overcome resistance to flow and thus maximize the productivity. We then turn the reservoir with infinite laterals in the horizontal plane on one of its sides so that the laterals are in a vertical plane. The maximum or the upper limit of productivity for the infinite laterals is obtained when the pressure drop in the laterals is negligible and hence they can then be modeled as an infinite conductivity fracture. We first present a rigorous derivation of the maximum dimensionless PI (J_d) for an infinite conductivity fracture as presented by Wattenbarger[23] *et al*. This result ($J_{d\max}$) is then used to obtain the maximum PI for a reservoir geometry used extensively in this research.

Again to estimate the theoretical lower limit of PI we use the known analytical result[24], which predicts the PI for a reservoir of arbitrary drainage area and shape and given as,

$$J = \frac{kh}{141.2B\mu} \frac{1}{\left(\frac{1}{2} \ln\left(\frac{4A}{\gamma C_A r_w^2} \right) + s \right)} \quad \text{... (3.1)}$$

where,

k = Permeability, md

h = Reservoir depth, ft

B = Oil formation volume factor

μ = Viscosity, cp

A = Drainage Area, ft ^{2}

γ = Euler's Constant

C_A = Dietz shape factor

r_w = Well bore radius, ft

s = skin factor

The above equation is essentially derived for a vertical well operating at pseudo-steady state. As in the case of determining the upper limit, we rotate the reservoir on one of its sides so that all the laterals are in the vertical plane. With such a rearrangement we can consider each lateral as a unique identity separated from the neighboring laterals in the reservoir by an imaginary no flow boundary. Then each block containing one lateral in the vertical plane surrounded by no flow boundaries on all sides can be assumed to represent a partially penetrating vertical well. Such a rearrangement is shown in Figure 3.1 for a ML well containing 2 laterals in the horizontal plane. Any partially penetrating well imparts a skin also known as the pseudo-skin factor. Cinco-Ley[25] *et al.* has published data for the skin effects of partially penetrating wells. The PI for a block containing a partially penetrating vertical well can be determined using the known values of Dietz' shape factor and pseudo-skin as given by Cinco-Ley. We expect, from basic reservoir engineering principles, that the sum of PI's for each of the block should be equal to the theoretical value of the least PI attainable by using the ML well architecture. However modeling the worst case behavior by introducing a no flow boundary between the laterals is not very intuitive and obvious.

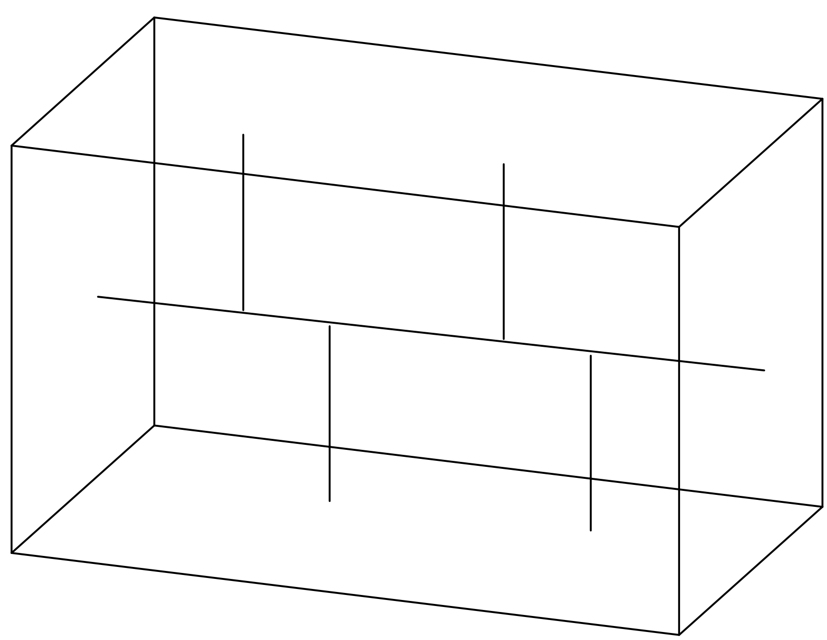

Figure 3.1 – Rearranged form of a horizontal well architecture

3.3 Upper Limit / Maximum Achievable PI

3.3.1 Infinite Conductivity Fracture PI

The PI attainable for an infinite conductivity fracture has been obtained by Watterbarger *et al*. In this section we present a rigorous derivation of the result for pseudo-steady state behavior. As mentioned earlier the flow into an infinite conductivity fracture is linear. Hence to model this physics of the phenomenon we use the linear diffusivity equation and obtain its solution for pseudo-steady state which requires a no flow outer boundary and constant rate inner boundary condition. The linear diffusivity equation has been presented in fluid flow texts. Consider a hydraulically fractured well in a rectangular geometry as shown in Figure 3.2. We use the equation as given below in field units. A rigorous derivation of the result obtained in the literature has been provided in the appendix.

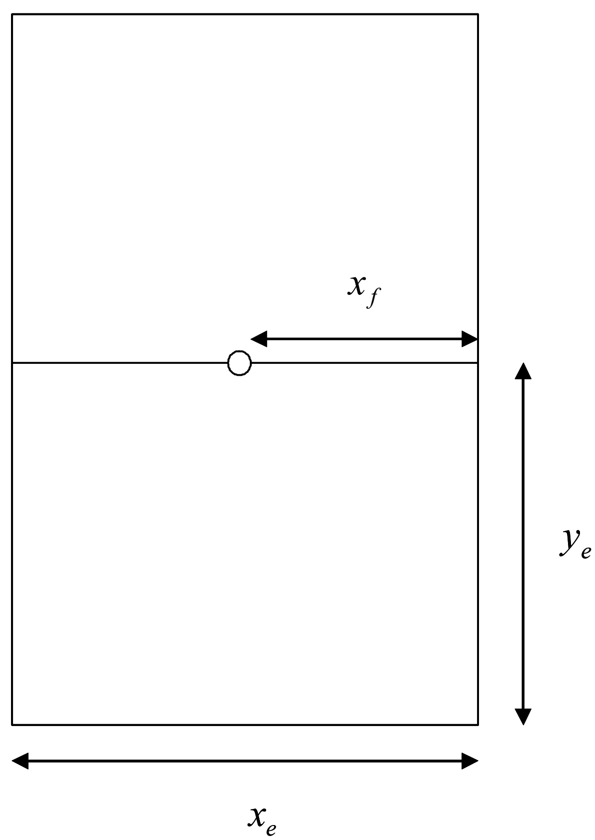

Figure 3.2 – Infinite conductivity fracture in a rectangular geometry

The maximum PI attainable for the case of an infinite fracture is

$$J_{CR} = \frac{kh}{141.2\,B\mu\left[\frac{\pi}{6}\left(\frac{y_e}{x_f}\right)\right]} \quad \text{……………………………………………………} \quad (3.2)$$

3.3.2 Application to ML Well Architecture

As mentioned earlier we rotate the reservoir on one of its sides so that the lateral structure can be modeled as an infinite conductivity fracture. This rearrangement of the horizontal laterals so that they lie in the vertical plane is shown in Figure 3.3. The correspondence between the dimensions of the original structure and the rearranged structure can be seen in figure and is given below,

$$x_h = x_f \quad \text{……………………………………………………………………..} \quad (3.3)$$

$$y_h = h \quad \text{……………………………………………………………………..} \quad (3.4)$$

$$h_h = y_e \quad \text{……………………………………………………………………..} \quad (3.5)$$

In eqn. 3.2 the term x_f, is the fracture half length. The fracture wings extend from the well bore to the lateral boundaries in the x-direction, and so x_f is equal to half the length of the reservoir in the x-direction. Similarly the term y_e is equal to half the length of the reservoir in the y-direction. This is seen in Figure 3.3. Hence, in order to

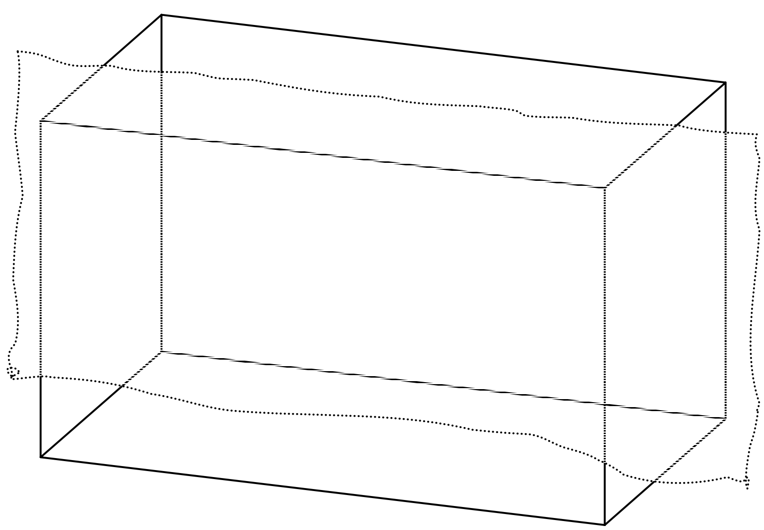

Figure 3.3 – Infinite laterals forming an infinite conductivity fracture in the vertical plane

determine the maximum PI for the ML well architecture the ratio $\left(\frac{y_e}{x_f}\right)$ in the infinite conductivity fracture solution can be replaced by the ratio of the lengths of the original reservoir in the y and x – directions as $\left(\frac{y_h}{x_h}\right)$. Hence the maximum PI for the case shown in Figure 3.3 is given by the following equation,

$$J = \frac{kh}{141.2\ B\mu}\left[\left(\frac{x_f}{y_e}\right)\frac{6}{\pi}\right] \quad \text{(3.6)}$$

The data used to evaluate the above expression are,

k = 0.1 mD

h = 2000 ft

x_e = 4000 ft

y_e = 110 ft

B = 1 .012 rb/stb

μ = 1.0 cp

$$J = \frac{0.1\times 2000}{141.2\times 1.012\times 1.0}\left[\left(\frac{4000}{110}\right)\frac{6}{\pi}\right] \quad \text{(3.7)}$$

$$J \approx 97 \text{ stbd/psia} \quad \text{(3.8)}$$

Hence the maximum PI of the ML well architecture is 97 stbd/psia.

3.4 Lower Limit for PI

3.4.1 Outline

We believe that a restriction in the form of a no flow boundary between neighboring laterals will be a good way to estimate the lower limit of productivity that can be delivered by the ML well architecture. Consider the Figure 3.1 shown earlier. In the rearranged vertical form the no flow boundary allows each lateral to be considered as a partially penetrating vertical well. The productivity of each well or block can be predicted by using a known analytical result from the literature as given by equation 3.1. This result accounts for the irregular shape of the reservoir, the well location and the skin due to a partially penetrating well. Reservoir engineering logic suggests that the sum of the productivity of all the blocks should be equal to the productivity of the ML well architecture. In fact the estimate by the analytical result should slightly under predict the ML well productivity as the laterals will normally drain the reservoir more uniformly than the set of partially penetrating vertical wells. However from the results shown in the next section we see that the present analytical tool is inadequate to predict the performance of ML wells as they more often than not tend to over-predict the PI in most cases analyzed.

Ideally the analytical result should be compared with the numerical solution of productivity for the reservoir geometry used. The reservoir considered is 4000 × 2000 × 110 feet in the x, y and z directions respectively. Rearrangement of the reservoir causes re-orientation of the dimensions in the y and z directions with the dimensions in the 3 co-ordinate directions now being 4000 × 110 × 2000 feet. Data for pseudo-skin and Dietz shape factor are not available for this geometry and hence we adopt a two step approach to investigate the ability of the current analytic tool to predict performance.

3.4.2 Step 1 - Numerical Analysis of Actual ML Well with Single Block Productivity

The first step is essentially a validation of the reservoir engineering principle that the sum of PI's for all blocks must be nearly equal to the PI of a ML well architecture. Herein we numerically simulate the performance of an 8 lateral and a 15 lateral structure in the original geometry. We then compare this performance with that of a single block which would be a subset of the rearranged ML well architecture. The geometry of the single block, the x-dimension, depends upon the number of laterals in the original ML well architecture. All the blocks have the same geometry, so the number of blocks is equal to the number of laterals considered. The results confirm that a single block of appropriate dimensions could be used to accurately predict the productivity of a large ML well.

The results for an 8 lateral structure are shown below. For a single block of appropriate dimensions (500 × 110 × 2000) the pseudo-steady state PI is 0.21. Hence for 8 vertical well this sums to 1.68 (Table 3.1). The productivity of an 8 lateral structure with dimensions 4000 × 110 × 2000 is observed to be 1.69 as shown in Table 3.2. Similarly the performance of a 15 lateral structure and the corresponding single block structure are compared in Tables 3.3 and 3.4.

Table 3.1 – Single block productivity for an 8 lateral structure subset

Time	Years	Wopr	Fopt	Fpr	Wbhp	J
days	years	stb/day	stb	psia	psia	stbd/psia
0	0.0	0	0	4,000	4,000	-
1	0.0	100	100	3,994	3,796	0.50
3	0.0	100	300	3,983	3,758	0.45
5	0.0	100	500	3,971	3,734	0.42
10	0.0	100	1,000	3,943	3,683	0.39
15	0.0	100	1,500	3,914	3,635	0.36
20	0.1	100	2,000	3,885	3,589	0.34
35	0.1	100	3,500	3,799	3,464	0.30
50	0.1	100	5,000	3,713	3,349	0.27
75	0.2	100	7,500	3,569	3,173	0.25
100	0.3	100	10,000	3,426	3,009	0.24
125	0.3	100	12,500	3,282	2,852	0.23
150	0.4	100	15,000	3,138	2,699	0.23
175	0.5	100	17,500	2,994	2,549	0.22
200	0.5	100	20,000	2,850	2,402	0.22
225	0.6	100	22,500	2,706	2,255	0.22
250	0.7	100	25,000	2,562	2,110	0.22
275	0.8	100	27,500	2,418	1,964	0.22
300	0.8	100	30,000	2,274	1,819	0.22
325	0.9	100	32,500	2,130	1,675	0.22
350	1.0	100	35,000	1,985	1,530	0.22
375	1.0	100	37,500	1,841	1,385	0.22
400	1.1	100	40,000	1,697	1,241	0.22
425	1.2	100	42,500	1,552	1,096	0.22
450	1.2	100	45,000	1,408	951	0.22
475	1.3	100	47,500	1,263	806	0.22
500	1.4	100	50,000	1,118	662	0.22
525	1.4	100	52,500	974	517	0.22
550	1.5	67	54,178	876	500	0.18
575	1.6	46	55,334	809	500	0.15
600	1.6	34	56,186	760	500	0.13

For a single block PI = 0.21

Hence for 8 vertical wells the PI = 0.21 × 8 = 1.68

Table 3.2-Productivity of an 8 lateral structure

Time	Years	Wopr	Fopt	Fpr	Wbhp	J
days	years	stb/day	Stb	psia	psia	stbd/psia
0	0.0	0	0	4,000	4,000	-
1	0.0	400	400	3,997	3,874	3.26
3	0.0	400	1,200	3,991	3,856	2.96
5	0.0	400	2,000	3,986	3,845	2.84
10	0.0	400	4,000	3,971	3,821	2.66
15	0.0	400	6,000	3,957	3,798	2.52
20	0.1	400	8,000	3,943	3,777	2.41
35	0.1	400	14,000	3,900	3,717	2.19
50	0.1	400	20,000	3,856	3,662	2.05
75	0.2	400	30,000	3,785	3,576	1.92
100	0.3	400	40,000	3,713	3,495	1.84
125	0.3	400	50,000	3,641	3,417	1.79
150	0.4	400	60,000	3,569	3,342	1.76
175	0.5	400	70,000	3,497	3,267	1.74
200	0.5	400	80,000	3,426	3,194	1.72
225	0.6	400	90,000	3,354	3,120	1.72
250	0.7	400	100,000	3,282	3,048	1.71
275	0.8	400	110,000	3,210	2,975	1.71
300	0.8	400	120,000	3,138	2,903	1.70
325	0.9	400	130,000	3,066	2,831	1.70
350	1.0	400	140,000	2,994	2,759	1.70
375	1.0	400	150,000	2,922	2,687	1.70
400	1.1	400	160,000	2,850	2,615	1.70
425	1.2	400	170,000	2,778	2,542	1.70
450	1.2	400	180,000	2,706	2,470	1.70
475	1.3	400	190,000	2,634	2,398	1.70
500	1.4	400	200,000	2,562	2,326	1.70
525	1.4	400	210,000	2,490	2,254	1.70
550	1.5	400	220,000	2,418	2,182	1.70
575	1.6	400	230,000	2,346	2,110	1.69
600	1.6	400	240,000	2,274	2,038	1.69

The PI of the 8 lateral structure compares very well with the 8 block PI’s

Table 3.3 – Single block productivity of a 15 lateral subset

Time	Years	Wopr	Fopt	Fpr	Wbhp	J
days	years	stb/day	stb	psia	psia	stbd/pspia
0	0.0	0	0	4,000	4,000	
1	0.0	50	50	3,995	3,876	0.42
3	0.0	50	150	3,984	3,850	0.37
5	0.0	50	250	3,973	3,829	0.35
10	0.0	50	500	3,946	3,782	0.30
15	0.0	50	750	3,919	3,737	0.27
20	0.1	50	1,000	3,892	3,694	0.25
35	0.1	50	1,750	3,812	3,578	0.21
50	0.1	50	2,500	3,731	3,471	0.19
75	0.2	50	3,750	3,596	3,309	0.17
100	0.3	50	5,000	3,462	3,157	0.16
125	0.3	50	6,250	3,327	3,011	0.16
150	0.4	50	7,500	3,192	2,870	0.16
175	0.5	50	8,750	3,057	2,730	0.15
200	0.5	50	10,000	2,922	2,593	0.15
225	0.6	50	11,250	2,787	2,456	0.15
250	0.7	50	12,500	2,652	2,320	0.15
275	0.8	50	13,750	2,517	2,184	0.15
300	0.8	50	15,000	2,382	2,048	0.15
325	0.9	50	16,250	2,247	1,913	0.15
350	1.0	50	17,500	2,112	1,777	0.15
375	1.0	50	18,750	1,976	1,642	0.15
400	1.1	50	20,000	1,841	1,506	0.15
425	1.2	50	21,250	1,706	1,371	0.15
450	1.2	50	22,500	1,570	1,235	0.15
475	1.3	50	23,750	1,435	1,100	0.15
500	1.4	50	25,000	1,299	964	0.15
525	1.4	50	26,250	1,164	828	0.15
550	1.5	50	27,500	1,028	693	0.15
575	1.6	50	28,750	892	557	0.15
600	1.6	36	29,649	795	500	0.12

Hence the productivity of 15 blocks = $0.15 \times 15 = 2.25$

Table 3.4 – Productivity of a 15 lateral structure

Time	Years	Wopr	Fopt	Fpr	Wbhp	J
days	years	stb/day	stb	psia	psia	stbd/psia
0	0.0	0	0	4,000	4,000	
1	0.0	200	200	3,999	3,963	5.63
3	0.0	200	600	3,996	3,957	5.17
5	0.0	200	1,000	3,993	3,952	4.88
10	0.0	200	2,000	3,986	3,940	4.38
15	0.0	200	3,000	3,978	3,929	4.02
20	0.1	200	4,000	3,971	3,918	3.75
35	0.1	200	7,000	3,950	3,889	3.27
50	0.1	200	10,000	3,928	3,861	2.98
75	0.2	200	15,000	3,892	3,819	2.73
100	0.3	200	20,000	3,856	3,779	2.58
125	0.3	200	25,000	3,821	3,741	2.50
150	0.4	200	30,000	3,785	3,703	2.45
175	0.5	200	35,000	3,749	3,666	2.42
200	0.5	200	40,000	3,713	3,630	2.40
225	0.6	200	45,000	3,677	3,593	2.39
250	0.7	200	50,000	3,641	3,557	2.38
275	0.8	200	55,000	3,605	3,521	2.37
300	0.8	200	60,000	3,569	3,485	2.37
325	0.9	200	65,000	3,533	3,449	2.37
350	1.0	200	70,000	3,497	3,413	2.37
375	1.0	200	75,000	3,461	3,377	2.36
400	1.1	200	80,000	3,425	3,341	2.36
425	1.2	200	85,000	3,390	3,305	2.36
450	1.2	200	90,000	3,354	3,269	2.36
475	1.3	200	95,000	3,318	3,233	2.36

Again from the above simulation results we see that the productivity of 15 identical blocks will slightly under predict the productivity of a ML well with 15 laterals Fig 3.4 shows a comparison of these simulation results and reinforce the belief that single block PI can be used to accurately predict the PI of the ML well architecture.

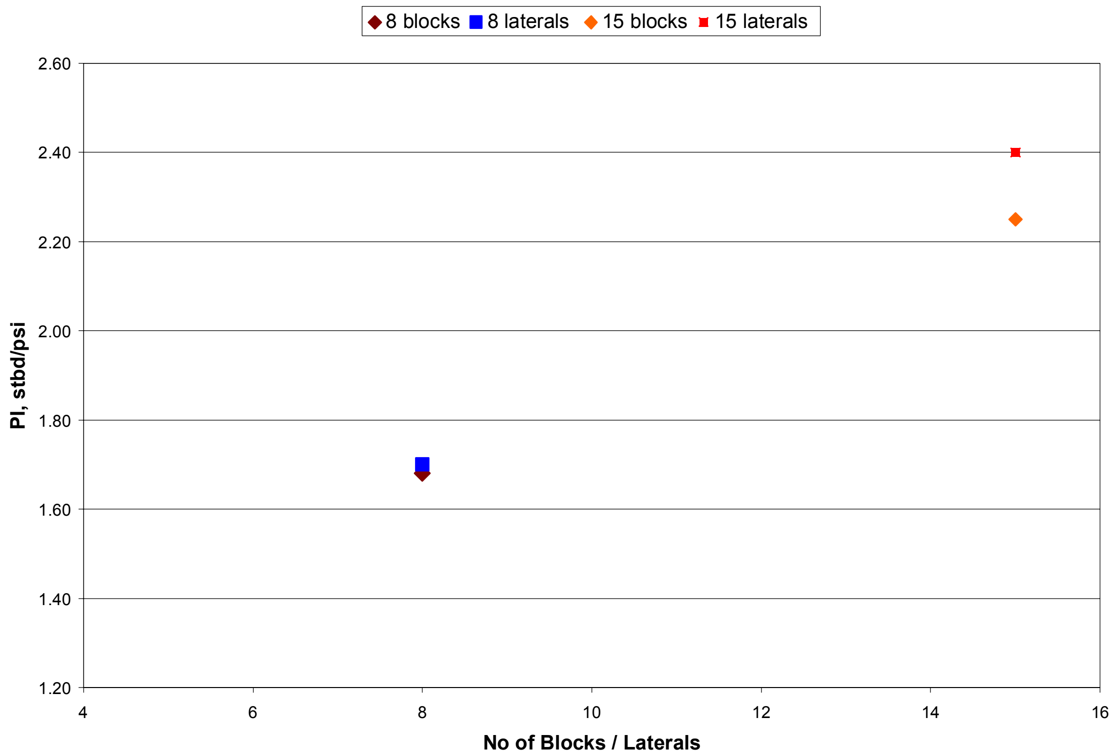

Figure 3.4 – Comparison of single block performance with the corresponding ML well structure

3.4.3 Step 2 – Analysis of Analytic and Numeric Solution for Well-Defined Geometry

In the second step the idea is to use the pseudo-skin and shape factor data published in the literature to evaluate the PI of a single block and compare it to the numerical solution of similar geometry containing a partially penetrating well. By doing so we can observe the results and comment whether the current tools are good enough to accurately predict the performance of a block which in turn predicts ML well performance. Dietz shape factor [24] is available for an aspect ratio of 1:5 with the well in the center. This geometry shown in Figure 3.5comes closest to the single block geometry of an 8 lateral structure subset and hence we choose this ratio for our computations. The dimensions used in the x and y directions are 500 ×100 feet with varying depths. We also perform the comparison of analytic and numeric solutions for the isotropic and anisotropic case. The anisotropy exits in the horizontal plane in the rearranged structure, in other words for the anisotropic case $k_x = k_z \neq k_y$. In all the cases analyzed we consider a vertical well with 50% penetration in the z-direction.

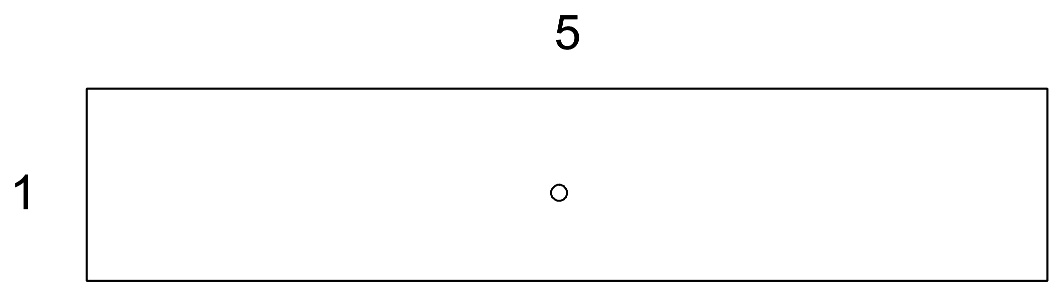

Figure 3.5– Simplest single block structure with a 5:1 ratio between its sides

Cinco-Ley *et. al.* have presented pseudo-skin data for partially penetrating wells for certain dimensionless variables such as $h_D = h / r_w$; z_w / h; h_w / h and h / r_w. The data is available for values of h_D equal to 100 and 1000. Hence we define cases such the dimensionless thickness h_D is equal to either of these values. Figure 3.6shows a partially penetrating well and significance of the values. Hence z_w / h is the elevation ratio while h_w / h is the completion ratio. In all the cases analyzed here we assume 50% penetration in the upper half of the reservoir. Hence the elevation ratio and the completion ratio is 0.75 and 0.5 in all the cases studied. The value of the dimensionless thickness depends upon the choice of the well bore radius. In order to match the available solutions from Cinco-Ley we use the following sets of values for reservoir depth and well bore radius as given in Table 3.5. The table also gives the corresponding value of pseudo-skin.

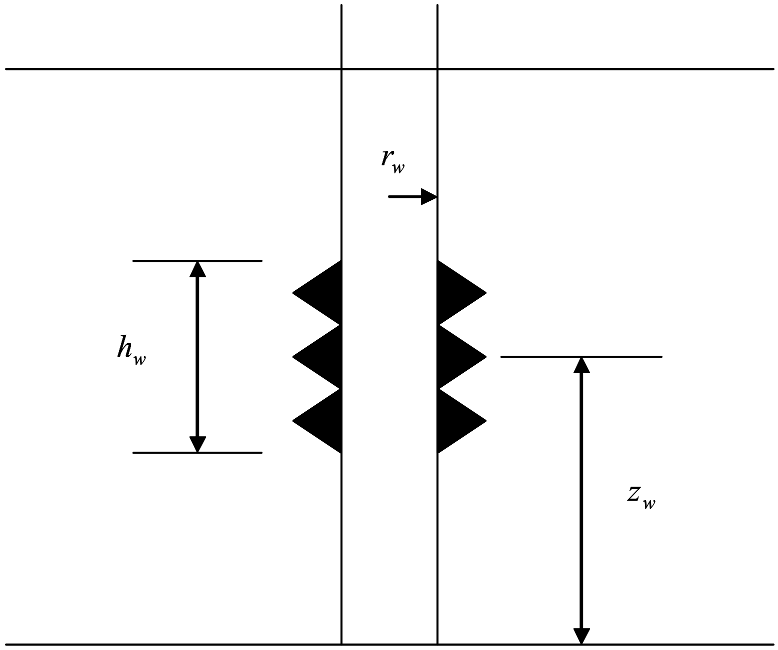

h_w = Completion Thickness

z_w = Elevation

Figure 3.6– Partially penetrating vertical well

Table 3.5 – Dimensionless height for Cinco pseudo-skin data

Depth, ft	Well bore Radius, ft	h_D	Skin, S
50	0.5	100	3.067
500	0.5	1000	5.467
1000	1	1000	5.467
1500	1.5	1000	5.467

Consider the first case when the depth is equal to 50 ft. The dimensions of the block are 500 × 100 × 50 in the three co-ordinate directions. As in all the other cases the drainage area to be used for the analytic solution is 500 × 100. For this drainage area with the well in the center the Dietz shape factor is 2.36. For a given depth corresponding values of well bore radius and skin are used. The equation used is,

$$J = \frac{kh}{141.2B\mu} \frac{1}{\left(\frac{1}{2} \ln \left(\frac{4A}{\gamma C_A r_w^2} \right) + s \right)} \quad \text{..........} (3.1)$$

Depending upon the permeability distribution in the reservoir the value of k will change for a isotropic and anisotropic reservoir. For the rearranged structure the permeability anisotropy exists in the x-y plane i.e. in the horizontal plane. For the purpose of this calculation we have used $k = \sqrt{k_x k_y}$ in anisotropic cases. For the isotropic case we assume the permeability to be equal to 1 in all directions.

Hence for a given reservoir configuration we have solutions for the isotropic as well as the anisotropic case. A comparison of the analytic and numeric results is shown in Table 3.6 for the isotropic case and Table 3.7 for the anisotropic case. These results are then plotted to in Figure 3.7and Figure 3.8 to show the deviation in the results with increasing depths.

Table 3.6 – Comparison of PI's for isotropic case

Reservoir Dimension	$J_{Analytical}$ Stbd/psia	$J_{Numerical}$ Stbd/psia
500 × 100 × 50	0.038	0.032
500 × 100 × 500	0.306	0.2
500 × 100 × 1000	0.644	0.296
500 × 100 × 1500	1.004	0.307

Table 3.7 – Comparison of PI's for anisotropic case

Reservoir Dimension	$J_{Analytical}$ Stbd/psia	$J_{Numerical}$ Stbd/psia
500 × 100 × 50	0.011	0.015
500 × 100 × 500	0.093	0.107
500 × 100 × 1000	0.199	0.183
500 × 100 × 1500	0.311	0.219

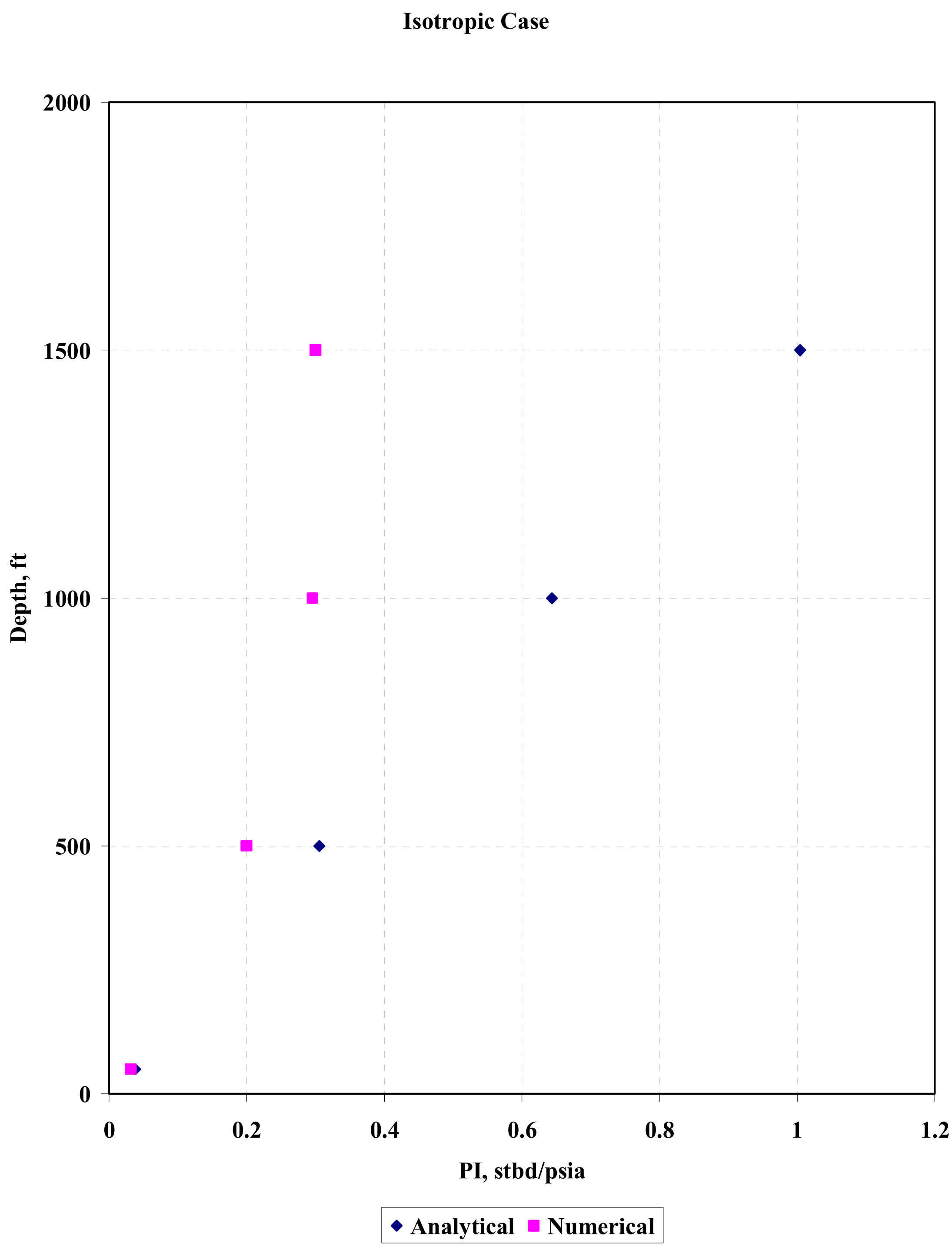

Figure 3.7 – Comparison of results for isotropic case

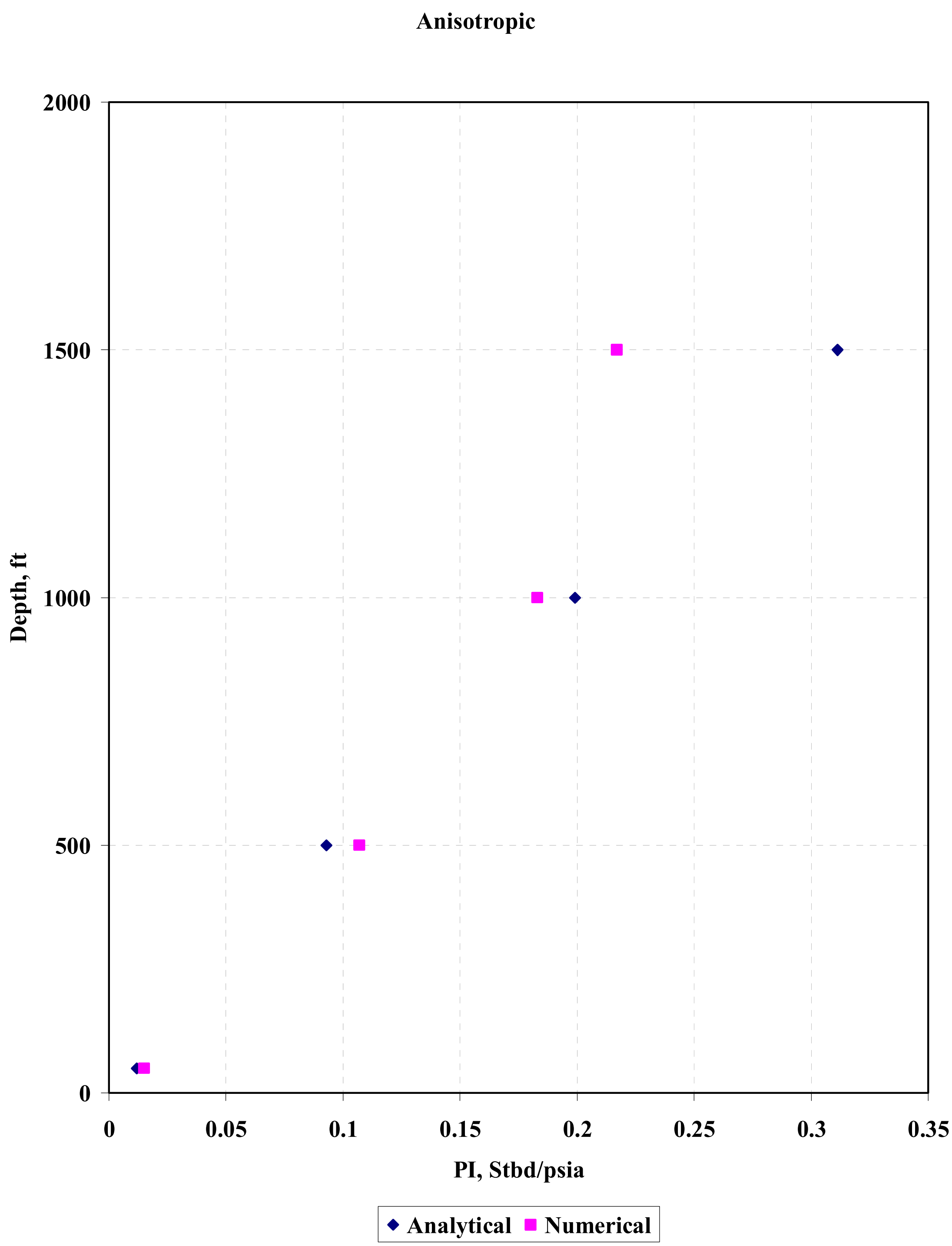

Figure 3.8 – Comparison of results for anisotropic case

3.4.4 Discussion of Results

From the results we can clearly see that the present analytical tool is not very effective in accurately predicting the productivity of a block containing a partially penetrating well. The analytical solution compares reasonable well with the numerical results at low depths. But at greater depths the analytical and numerical solutions diverge for both the isotropic and anisotropic case.

CHAPTER IV
PRELIMINARY ANALYSIS OF PROPOSED ARCHITECTURE FOR SYNTHETIC CASES

4.1 Parameters to be Analyzed

In this chapter we simulate synthetic cases to study the effect of various parameters on the performance of ML wells. A base case is set up containing a ML well architecture described earlier. Single phase flow of dry oil, which contains no dissolved gases, is considered in this parametric analysis. The parameters we wish to investigate are essentially related to the design of the architecture and primary reservoir properties that affect the flow of the fluids in the reservoir.

Branch Density & Extent of Penetration – The cost of a ML well will depend greatly upon the number of laterals to be drilled and extent of their penetration into the bulk of the reservoir. Drilling any more laterals than absolutely necessary puts greater burden on the cash flow. On the other hand fewer laterals might not utilize the full benefits of the larger reservoir exposure offered by ML wells. It is expected that initially adding a lateral to the structure will continuously add production but after a certain extent the addition of each extra lateral will not significantly add to the total production. In such a case the excess laterals become redundant. Also it might be beneficial to drill the laterals only to a certain extent into the reservoir rather than all the way to the lateral boundary. We wish to address such issues through this analysis. The aim in designing the architecture is to drill an optimum number of laterals with an optimum penetration extent so that the benefit to cost ratio of the well, which is nothing but the stock tank barrels of oil produced per dollar spent, is maximized. Hence we choose branch density and penetration extent as the investigative parameters at the outset.

Permeability Variations – The flow into the laterals will be normally linear and perpendicular. The laterals are considered to be only in the horizontal direction and hence the permeability in the z direction plays an important role in the inflow to the laterals. We compare the effect of permeability variation for a given lateral structure.

4.2 Reservoir Geometry and Properties

A homogeneous rectangular reservoir is simulated. The dimensions of the reservoir in the 3 co-ordinate directions are 2000 × 4000 × 110 respectively. The mother bore is placed at the middle of the reservoir in the z-direction. While the laterals form an alternating mesh of perforated slim holes connected to the mother bore. The base case analyzed is anisotropic, so that the permeability in the horizontal and vertical direction is not the same. A 21 × 62 × 11 grid is used. The other important input properties are shown in the Table 4.1 below.

Table 4.1 – Base case reservoir properties

Grid Size	21 × 62 × 11
Reservoir Size	2000 × 4000 × 110
Permeability (mD)	Anisotropic
$k_x = k_y$	1.00
k_z	0.10
Porosity	0.3

4.3 Simulation Cases

To analyze density effects of laterals we simulate a 60, 30, 15 and a 4 – lateral structure for complete penetration from the mother bore to the lateral boundary. This is followed by simulation for the lateral partial penetration assuming they penetrate out to an extent of 45% and 75% of lateral dimension. Finally to observe permeability effects we simulate the base case assuming isotropic permeability in the reservoir.

4.4 Simulation Results

4.4.1 Branch Density and Partial Penetration Effects

A summary of some key results for branch density effects is given in Table 4.2. From the table we see that the cumulative production for a structure with 60 laterals is 0.5520 MMSTB, while the cumulative production from a 4 - lateral structure is 0.5505 MMSTB. The difference of about 1500 STB indicates that the same reservoir can be depleted to nearly the same extent by using much fewer laterals. In other words after a certain number increasing the number of laterals does not increase the cumulative production by a large amount. The only noticeable difference between using a very high number of laterals as compared to using an optimum is in the time required to attain a certain amount of cumulative production. For example the time to obtain 550,000 STB of cumulative production from a 60 and a 4 lateral structure would be 287 days and 1000 days respectively.

In all the runs mentioned above the bottom hole flowing pressure was allowed to fall to 14.7 psia. These cases were simulated again, but this time the bottom hole flowing pressure is set to not decrease below 1000 psia. The corresponding results are tabulated in Table 2 - B. Again the difference in cumulative for 60 and 4 laterals is very small and the basic difference is in the time distribution of the production. The results of the simulation for the effect of density are shown in Tables 4.3 – 4.6. Figure 4.1 shows a variation in bottomhole pressure with the number of laterals.

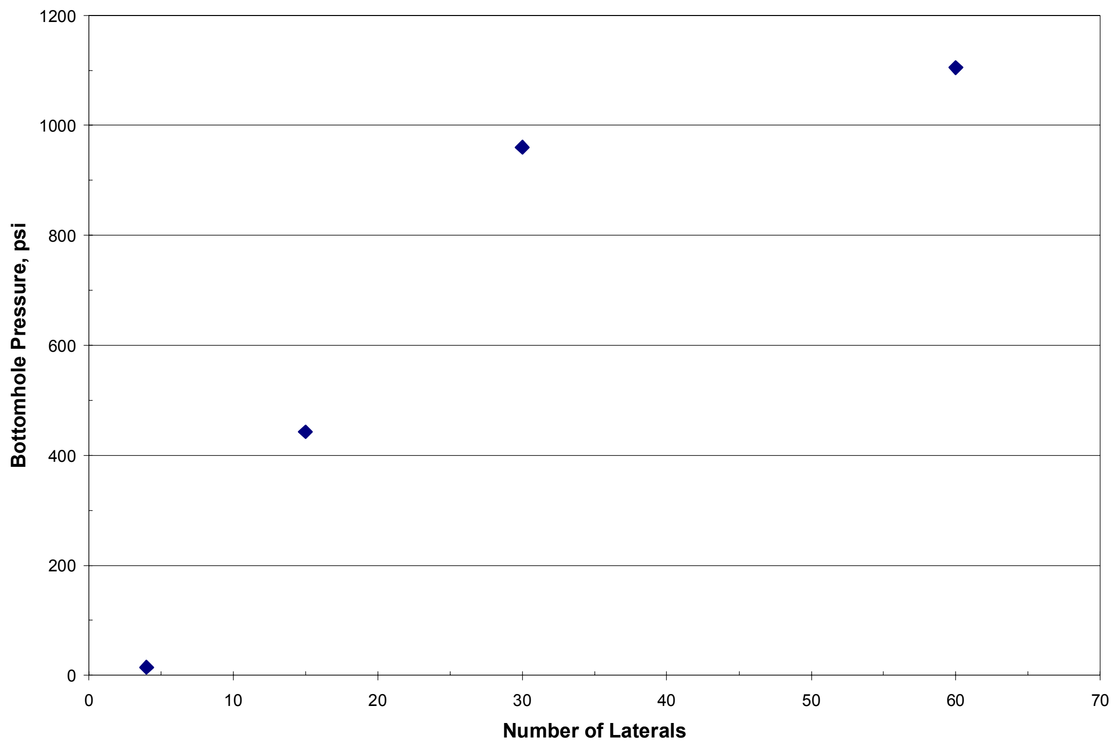

Figure 4.1 – A much lower bottomhole pressure is needed when using fewer laterals, increasing the possibility of borehole collapse, sand production, water coning.

Table 4.2 - Summary of simulation results

Well Structure	Cum Prod.	Field Pressure	BHP
(No. of Laterals)	stb	psia	psia
[A] Base Case Runs			
60	552,030	18	0
30	552,048	18	14.7
15	552,041	18	14.7
4	550,539	29	14.7
[B] Base Case Runs (BHP = 1000 PSIA)			
60	416,055	1,003	0
30	416,049	1,003	0
4	414,971	1,011	1,000

Table 4.3 – Productivity of a 60 lateral structure

Time	Years	Wopr	Fopt	Fpr	Wbhp	J
days	years	stb/day	stb	psia	psia	stbd/psia
0.0	0.0	0.0	0.0	4000.0	4000.0	-
1.0	0.0	3818.2	3818.2	3972.5	3838.6	28.5
3.0	0.0	3818.2	11454.5	3917.8	3774.7	26.7
5.0	0.0	3818.2	19090.9	3863.0	3718.9	26.5
10.0	0.0	3818.2	38181.8	3726.1	3581.7	26.4
15.0	0.0	3818.2	57272.7	3589.1	3444.6	26.4
20.0	0.1	3818.2	76363.6	3452.0	3307.4	26.4
35.0	0.1	3818.2	133636.3	3040.4	2895.7	26.4
50.0	0.1	3818.2	190909.0	2628.3	2483.4	26.3
75.0	0.2	3818.2	286363.5	1940.4	1795.2	26.3
100.0	0.3	3818.2	381818.0	1251.1	1105.6	26.2
150.0	0.4	3086.5	536140.8	133.4	14.7	-
200.0	0.5	287.5	550515.1	29.1	14.7	-
300.0	0.8	14.4	551952.1	18.6	14.7	-
400.0	1.1	0.7	552024.4	18.1	14.7	-
500.0	1.4	0.1	552029.8	18.1	14.7	-
600.0	1.6	0.0	552030.1	18.1	14.7	-
700.0	1.9	0.0	552030.1	18.1	0.0	-
800.0	2.2	0.0	552030.1	18.1	0.0	-
900.0	2.5	0.0	552030.1	18.1	0.0	-
1000.0	2.7	0.0	552030.1	18.1	0.0	-

Table 4.4 – Productivity of a 30 lateral structure

Time	Years	Wopr	Fopt	Fpr	Wbhp	J
days	years	stb/day	stb	psia	Psia	stbd/psia
0	0.0	0.0	0	4,000.0	4,000.0	-
1	0.0	3,818.2	3,818	3,972.6	3,706.7	14.4
3	0.0	3,818.2	11,455	3,917.9	3,634.5	13.5
5	0.0	3,818.2	19,091	3,863.1	3,576.9	13.3
10	0.0	3,818.2	38,182	3,726.2	3,438.7	13.3
15	0.0	3,818.2	57,273	3,589.2	3,301.0	13.3
20	0.1	3,818.2	76,364	3,452.1	3,163.6	13.2
35	0.1	3,818.2	133,636	3,040.5	2,751.4	13.2
50	0.1	3,818.2	190,909	2,628.4	2,338.8	13.2
75	0.2	3,818.2	286,364	1,940.5	1,650.2	13.2
100	0.3	3,818.2	381,818	1,251.2	960.3	13.1
150	0.4	2,817.5	522,695	231.1	14.7	-
200	0.5	484.3	546,911	55.4	14.7	-
300	0.8	46.4	551,549	21.7	14.7	-
400	1.1	4.5	551,996	18.5	14.7	-
500	1.4	0.5	552,042	18.1	14.7	-
600	1.6	0.0	552,047	18.1	14.7	-
700	1.9	0.0	552,048	18.1	14.7	-
800	2.2	0.0	552,048	18.1	14.7	-
900	2.5	0.0	552,048	18.1	14.7	-
1000	2.7	0.0	552,048	18.1	14.7	-

Table 4.5 - Productivity of a 15 lateral structure

Time	Years	Wopr	Fopt	Fpr	Wbhp	J
days	years	stb/day	stb	psia	psia	stbd/psia
0	0.0	0.0	0	4,000.0	4,000.0	-
1	0.0	3,818.2	3,818	3,972.9	3,295.8	5.6
3	0.0	3,818.2	11,455	3,918.2	3,166.5	5.1
5	0.0	3,818.2	19,091	3,863.4	3,092.1	5.0
10	0.0	3,818.2	38,182	3,726.5	2,942.4	4.9
15	0.0	3,818.2	57,273	3,589.5	2,799.8	4.8
20	0.1	3,818.2	76,364	3,452.4	2,659.5	4.8
35	0.1	3,818.2	133,636	3,040.9	2,242.6	4.8
50	0.1	3,818.2	190,909	2,628.8	1,826.9	4.8
75	0.2	3,818.2	286,364	1,940.8	1,135.2	4.7
100	0.3	3,818.2	381,818	1,251.4	443.0	4.7
150	0.4	2,141.5	488,894	476.3	14.7	-
200	0.5	788.0	528,292	190.5	14.7	-
300	0.8	181.7	546,464	58.6	14.7	-
400	1.1	42.5	550,715	27.7	14.7	-
500	1.4	10.1	551,722	20.4	14.7	-
600	1.6	2.4	551,964	18.7	14.7	-
700	1.9	0.6	552,022	18.2	14.7	-
800	2.2	0.1	552,036	18.1	14.7	-
900	2.5	0.0	552,040	18.1	14.7	-
1000	2.7	0.0	552,041	18.1	14.7	-

Table 4.6 - Productivity of a 4 lateral structure

Time	Years	Wopr	Fopt	Fpr	Wbhp	J
days	years	stb/day	stb	psia	psia	stbd/psia
0	0.0	0.0	0	4,000.0	4,000.0	-
1	0.0	3,818.2	3,818	3,973.5	2,341.4	2.3
3	0.0	3,818.2	11,455	3,918.9	1,993.4	2.0
5	0.0	3,818.2	19,091	3,864.2	1,817.9	1.9
10	0.0	3,818.2	38,182	3,727.3	1,528.4	1.7
15	0.0	3,818.2	57,273	3,590.4	1,285.4	1.7
20	0.1	3,818.2	76,364	3,453.3	1,064.4	1.6
35	0.1	3,818.2	133,636	3,041.5	477.6	1.5
50	0.1	3,701.5	189,159	2,641.8	14.7	-
75	0.2	2,701.4	256,694	2,154.9	14.7	-
100	0.3	2,072.3	308,502	1,781.0	14.7	-
150	0.4	1,385.1	377,756	1,280.7	14.7	-
200	0.5	965.2	426,017	931.6	14.7	-
300	0.8	539.3	479,945	541.1	14.7	-
400	1.1	306.9	510,631	318.6	14.7	-
500	1.4	175.9	528,219	191.1	14.7	-
600	1.6	101.1	538,329	117.7	14.7	-
700	1.9	58.2	544,147	75.4	14.7	-
800	2.2	33.5	547,498	51.1	14.7	-
900	2.5	19.3	549,427	37.1	14.7	-
1000	2.7	11.1	550,539	29.1	14.7	-

Further results for partial penetration of laterals are shown in Tables 4.7 – 4.9. Here we compare partial penetration effects using 2 to 30 - laterals. A comparison of results shows that using 4 laterals produces just as well as 30 - laterals. However a comparison of production from 4 and 2 - laterals indicates a significant difference in cumulative production. This is observed even when the 4 - lateral structure penetrated to only 45% while the 2 lateral structure penetrated to about 73%. Also the time taken to produce the same amount of reservoir fluids is much less for the 4 – laterals case with 45% penetration thus increasing the economy of operation.

Table 4.7- Productivity of a 30 lateral structure with 45% penetration

Time	Years	Wopr	Fopt	Fpr	Wbhp	J
days	years	stb/day	stb	psia	psia	stbd/psia
0	0.0	0.0	0	4,000	4,000	-
1	0.0	3,818.2	3,818	3,972	3,302	5.7
4	0.0	3,818.2	15,273	3,890	3,106	4.9
13	0.0	3,818.2	49,636	3,643	2,724	4.2
25	0.1	3,818.2	95,455	3,314	2,302	3.8
50	0.1	3,818.2	190,909	2,627	1,546	3.5
75	0.2	3,430.8	276,680	2,009	1,000	3.4
100	0.3	2,003.1	326,756	1,647	1,000	3.1
200	0.5	340.8	399,892	1,119	1,000	2.9
300	0.8	61.7	412,979	1,024	1,000	2.5
305	0.8	55.7	413,257	1,022	1,000	2.5
310	0.8	50.3	413,509	1,020	1,000	2.5
315	0.9	45.5	413,736	1,018	1,000	2.4
320	0.9	41.1	413,942	1,017	1,000	2.4
325	0.9	37.1	414,128	1,016	1,000	2.3
337.5	0.9	29.4	414,496	1,013	1,000	2.2
350	1.0	23.2	414,785	1,011	1,000	2.1
400	1.1	9.9	415,410	1,006	1,000	1.5
500	1.4	1.8	415,786	1,004	1,000	-
600	1.6	0.3	415,853	1,003	1,000	-
700	1.9	0.1	415,865	1,003	1,000	-
800	2.2	0.0	415,867	1,003	1,000	-
900	2.5	0.0	415,867	1,003	1,000	-
1000	2.7	0.0	415,867	1,003	1,000	-

Table 4.8 – Productivity of a 4 lateral structure with 45% penetration in the reservoir

Time	Years	Wopr	Fopt	Fpr	Wbhp	J
days	years	stb/day	stb	psia	psia	stbd/psia
0	0.0	0	0	4,000	4000	-
1	0.0	2,305	2,305	3,984	1000	0.77
3	0.0	1,953	6,211	3,956	1000	0.66
5	0.0	1,843	9,898	3,929	1000	0.63
10	0.0	1,716	18,478	3,868	1000	0.60
15	0.0	1,635	26,655	3,809	1000	0.58
50	0.1	1,353	76,606	3,450	1000	0.55
100	0.3	1,100	134,554	3,034	1000	0.54
200	0.5	746	221,247	2,409	1000	0.53
300	0.8	512	280,501	1,982	1000	0.52
400	1.1	354	321,376	1,687	1000	0.52
500	1.4	246	349,749	1,482	1000	0.51
600	1.6	172	369,529	1,339	1000	0.51
625	1.7	157	373,462	1,311	1000	0.51
650	1.8	144	377,059	1,284	1000	0.51
675	1.8	132	380,349	1,261	1000	0.50
700	1.9	120	383,359	1,239	1000	0.50
725	2.0	110	386,112	1,219	1000	0.50
750	2.1	101	388,631	1,201	1000	-
775	2.1	92	390,938	1,184	1000	-
800	2.2	84	393,047	1,169	1000	-
900	2.5	59	399,847	1,120	1000	-
1000	2.7	42	404,629	1,085	1000	-

Table 4.9 – Productivity of a 2 lateral structure with 73 % penetration

Time	Years	Wopr	Fopt	Fpr	Wbhp	J
Days	years	stb/day	stb	psia	psia	stbd/psia
0	0.0	0	0	4,000	4000	-
1	0.0	1,765	1,765	3,988	1000	0.59
3	0.0	1,385	4,535	3,968	1000	0.47
5	0.0	1,253	7,040	3,950	1000	0.42
10	0.0	1,100	12,540	3,910	1000	0.38
50	0.1	772	46,477	3,667	1000	0.29
75	0.2	699	63,950	3,541	1000	0.28
100	0.3	647	80,119	3,425	1000	0.27
200	0.5	516	136,038	3,023	1000	0.26
300	0.8	428	181,985	2,692	1000	0.25
400	1.1	358	220,296	2,416	1000	0.25
500	1.4	299	252,319	2,185	1000	0.25
600	1.6	250	279,096	1,992	1000	0.25
700	1.9	209	301,490	1,831	1000	0.25
800	2.2	175	320,217	1,695	1000	-
900	2.5	146	335,878	1,582	1000	-
925	2.5	140	339,375	1,557	1000	-
950	2.6	134	342,720	1,533	1000	-
975	2.7	128	345,918	1,510	1000	-
1000	2.7	122	348,976	1,487	1000	-

4.4.2 Permeability

Permeability is perhaps the most important reservoir property that has a significant effect on the performance of multilateral wells. This is amply noticeable from the simulation results for isotropic and anisotropic reservoirs. The value of permeability used for isotropic reservoirs is 1 md while for the anisotropic reservoir a k_v/k_h ratio of 0.1 is used with a horizontal permeability of 1 md.

For both isotropic and anisotropic reservoirs the results show that as we decrease the branch density by half the PI also decreases by more than half. For example from the table we see that for an isotropic reservoir with a 60 – lateral structure the PI is 74 STBD/psia, while for a 30 – lateral structure the PI is 33 STBD/psia. This indicates a reduction of more than 50% in the PI. This trend is also observed when we reduce the branch density even further. Similar variation of results is also observed for an anisotropic reservoir though a much lower PI is achieved for a vertical to horizontal permeability ratio of 0.1.

The cumulative production from an isotropic reservoir is comparable for a structure with 60 – laterals and with 4 – laterals. However for the k_v/k_h ratio of 0.1 the cumulative production from a 4 – lateral structure is only 0.3085 MMSTB while it is 0.3818 MMSTB for a 15 – lateral structure. This shows that for a large permeability variation in the two directions the capacity to produce the fluids is lower and more time will be required to produce the same amount. The results are shown in Tables 4.10 – 4.15.Comparison of the PI for the two cases is shown in Figure 4.2

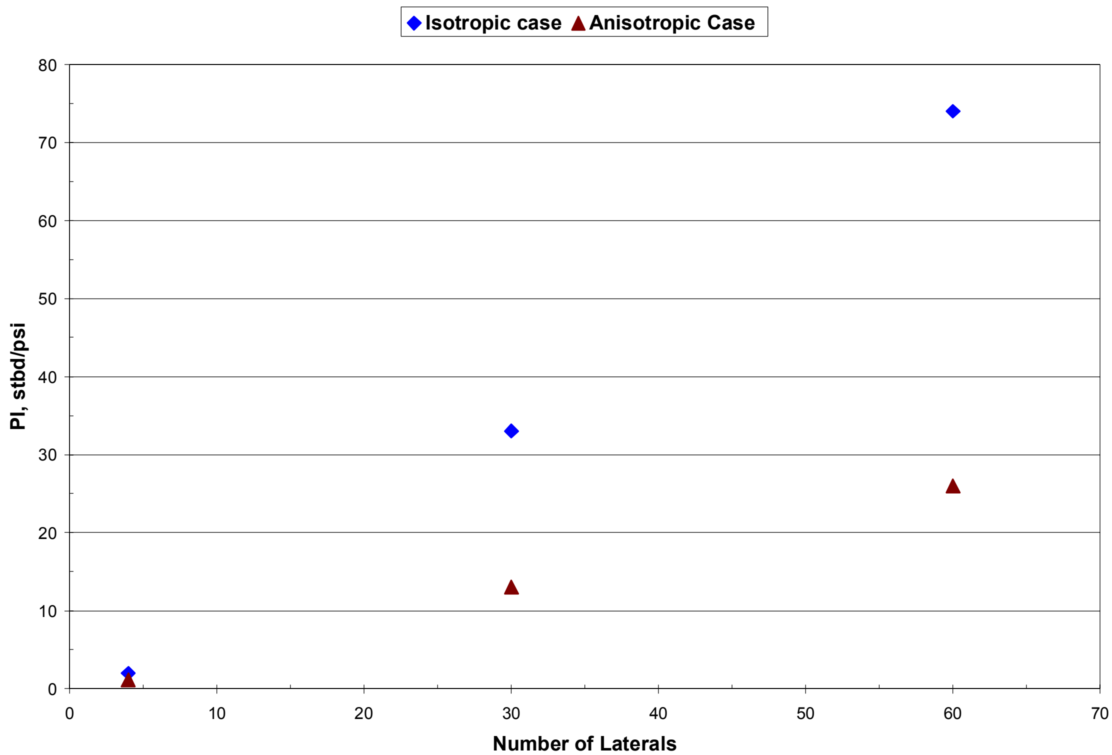

Figure 4.2 – Productivity of the ML well architecture decreases significantly (by 50%) as we go from an isotropic reservoir to an anisotropic reservoir

Table 4.10 – Isotropic reservoir productivity with a 60 lateral structure

Time	Years	Wopr	Fopt	Fpr	Wbhp	J
Days	years	stb/day	stb	psia	psia	stbd/psia
0	0.0	0	0	4,000	4,000	-
1	0.0	3,818	3,818	3,973	3,922	76.1
3	0.0	3,818	11,455	3,918	3,867	74.9
5	0.0	3,818	19,091	3,863	3,812	74.7
10	0.0	3,818	38,182	3,726	3,675	74.6
15	0.0	3,818	57,273	3,589	3,538	74.6
20	0.1	3,818	76,364	3,452	3,401	74.5
50	0.1	3,818	190,909	2,628	2,576	74.4
100	0.3	3,818	381,818	1,250	1,198	74.1
125	0.3	1,273	413,653	1,019	1,000	65.4
150	0.4	83	415,724	1,004	1,000	18.6
175	0.5	6	415,862	1,003	1,000	1.6
200	0.5	0	415,871	1,003	1,000	0.1
225	0.6	0	415,871	1,003	1,000	0.0
250	0.7	0	415,871	1,003	1,000	0.0
275	0.8	0	415,871	1,003	1,000	-
300	0.8	0	415,871	1,003	1,000	-
400	1.1	0	415,871	1,003	0	-
500	1.4	0	415,871	1,003	0	-
600	1.6	0	415,871	1,003	0	-
700	1.9	0	415,871	1,003	0	-
800	2.2	0	415,871	1,003	0	-
900	2.5	0	415,871	1,003	0	-
1000	2.7	0	415,871	1,003	0	-

Table 4.11 – Isotropic reservoir productivity with a 30 lateral structure

Time	Years	Wopr	Fopt	Fpr	Wbhp	J
Days	years	stb/day	stb	psia	psia	stbd/psia
0	0.0	0	0	4,000	4,000	-
1	0.0	3,818	3,818	3,973	3,867	36.0
3	0.0	3,818	11,455	3,918	3,807	34.4
5	0.0	3,818	19,091	3,863	3,751	34.0
10	0.0	3,818	38,182	3,726	3,613	33.8
15	0.0	3,818	57,273	3,589	3,476	33.7
20	0.1	3,818	76,364	3,452	3,338	33.6
35	0.1	3,818	133,636	3,040	2,926	33.6
50	0.1	3,818	190,909	2,628	2,514	33.5
75	0.2	3,818	286,364	1,939	1,825	33.5
100	0.3	3,818	381,818	1,250	1,135	33.4
125	0.3	1,171	411,100	1,038	1,000	30.9
150	0.4	163	415,181	1,008	1,000	19.4
175	0.5	24	415,769	1,004	1,000	5.7
200	0.5	4	415,858	1,003	1,000	1.0
300	0.8	0	415,871	1,003	1,000	0.0
400	1.1	0	415,871	1,003	1,000	0.0
500	1.4	0	415,871	1,003	0	-
600	1.6	0	415,871	1,003	0	-
700	1.9	0	415,871	1,003	0	-
800	2.2	0	415,871	1,003	0	-
900	2.5	0	415,871	1,003	0	-
1000	2.7	0	415,871	1,003	0	-

Table 4.12 – Isotropic reservoir productivity with a 4 lateral structure

Time	Years	Wopr	Fopt	Fpr	Wbhp	J
days	years	stb/day	stb	psia	psia	stbd/psia
0	0.0	0	0	4,000	4,000	-
1	0.0	3,818	3,818	3,973	3,055	4.16
3	0.0	3,818	11,455	3,918	2,756	3.29
5	0.0	3,818	19,091	3,863	2,558	2.93
10	0.0	3,818	38,182	3,726	2,233	2.56
15	0.0	3,818	57,273	3,589	1,981	2.37
20	0.1	3,818	76,364	3,452	1,768	2.27
35	0.1	3,818	133,636	3,040	1,245	2.13
50	0.1	3,358	184,013	2,677	1,000	2.00
75	0.2	2,317	241,934	2,260	1,000	1.84
100	0.3	1,680	283,929	1,957	1,000	1.76
125	0.3	1,241	314,952	1,733	1,000	1.69
150	0.4	927	338,128	1,566	1,000	1.64
175	0.5	699	355,606	1,439	1,000	1.59
200	0.5	531	368,891	1,343	1,000	1.55
300	0.8	190	397,722	1,135	1,000	1.41
400	1.1	74	408,512	1,057	1,000	1.29
500	1.4	30	412,815	1,026	1,000	1.16
600	1.6	13	414,631	1,013	1,000	1.02
700	1.9	5	415,377	1,007	1,000	0.73
800	2.2	2	415,681	1,005	1,000	0.43
900	2.5	1	415,804	1,004	1,000	0.21
1000	2.7	0	415,855	1,004	1,000	0.10

Table 4.13 – Anisotropic reservoir productivity with a 60 lateral structure

Time	Years	Wopr	Fopt	Fpr	Wbhp	J
days	years	stb/day	stb	psia	psia	stbd/psia
0	0.0	0	0	4,000.0	4,000.0	-
1	0.0	3,818	3,818	3,972.5	3,838.6	28.51
3	0.0	3,818	11,455	3,917.8	3,774.7	26.69
5	0.0	3,818	19,091	3,863.0	3,718.9	26.50
10	0.0	3,818	38,182	3,726.1	3,581.7	26.44
15	0.0	3,818	57,273	3,589.1	3,444.6	26.42
20	0.1	3,818	76,364	3,452.0	3,307.4	26.41
35	0.1	3,818	133,636	3,040.4	2,895.7	26.38
50	0.1	3,818	190,909	2,628.3	2,483.4	26.35
75	0.2	3,818	286,364	1,940.4	1,795.2	26.29
100	0.3	3,818	381,818	1,251.1	1,105.6	26.24
150	0.4	3,086	536,141	133.4	14.7	26.00
200	0.5	287	550,515	29.1	14.7	20.00
300	0.8	14	551,952	18.6	14.7	3.64
400	1.1	1	552,024	18.1	14.7	-
500	1.4	0	552,030	18.1	14.7	-
600	1.6	0	552,030	18.1	14.7	-
700	1.9	0	552,030	18.1	0.0	-
800	2.2	0	552,030	18.1	0.0	-
900	2.5	0	552,030	18.1	0.0	-
1000	2.7	0	552,030	18.1	0.0	-

Table 4.14 - Anisotropic reservoir productivity with a 30 lateral structure

Time	Years	Wopr	Fopt	Fpr	Wbhp	J
days	years	stb/day	stb	psia	psia	stbd/psia
0	0.0	0	0	4,000.0	4,000.0	-
1	0.0	3,818	3,818	3,972.6	3,706.7	14.4
3	0.0	3,818	11,455	3,917.9	3,634.5	13.5
5	0.0	3,818	19,091	3,863.1	3,576.9	13.3
10	0.0	3,818	38,182	3,726.2	3,438.7	13.3
15	0.0	3,818	57,273	3,589.2	3,301.0	13.3
20	0.1	3,818	76,364	3,452.1	3,163.6	13.2
35	0.1	3,818	133,636	3,040.5	2,751.4	13.2
50	0.1	3,818	190,909	2,628.4	2,338.8	13.2
75	0.2	3,818	286,364	1,940.5	1,650.2	13.2
100	0.3	3,818	381,818	1,251.2	960.3	13.1
150	0.4	2,818	522,695	231.1	14.7	13.0
200	0.5	484	546,911	55.4	14.7	11.9
300	0.8	46	551,549	21.7	14.7	6.6
400	1.1	4	551,996	18.5	14.7	1.2
500	1.4	0	552,042	18.1	14.7	0.1
600	1.6	0	552,047	18.1	14.7	0.0
700	1.9	0	552,048	18.1	14.7	0.0
800	2.2	0	552,048	18.1	14.7	0.0
900	2.5	0	552,048	18.1	14.7	0.0
1000	2.7	0	552,048	18.1	14.7	0.0

Table 4.15 – Anisotropic reservoir productivity with a 4 lateral structure

Time	Years	Wopr	Fopt	Fpr	Wbhp	J
days	years	stb/day	stb	psia	psia	stbd/psia
0	0.0	0	0	4,000.0	4,000.0	-
1	0.0	3,818	3,818	3,973.5	2,341.4	2.34
3	0.0	3,818	11,455	3,918.9	1,993.4	1.98
5	0.0	3,818	19,091	3,864.2	1,817.9	1.87
10	0.0	3,818	38,182	3,727.3	1,528.4	1.74
15	0.0	3,818	57,273	3,590.4	1,285.4	1.66
20	0.1	3,818	76,364	3,453.3	1,064.4	1.60
35	0.1	3,818	133,636	3,041.5	477.6	1.49
50	0.1	3,701	189,159	2,641.8	14.7	1.41
75	0.2	2,701	256,694	2,154.9	14.7	1.26
100	0.3	2,072	308,502	1,781.0	14.7	1.17
150	0.4	1,385	377,756	1,280.7	14.7	1.09
200	0.5	965	426,017	931.6	14.7	1.05
300	0.8	539	479,945	541.1	14.7	1.02
400	1.1	307	510,631	318.6	14.7	1.01
500	1.4	176	528,219	191.1	14.7	1.00
600	1.6	101	538,329	117.7	14.7	0.98
700	1.9	58	544,147	75.4	14.7	0.96
800	2.2	34	547,498	51.1	14.7	0.92
900	2.5	19	549,427	37.1	14.7	0.86
1000	2.7	11	550,539	29.1	14.7	0.77

4.4.3 Grid Refinement

The most common technique to establish the numerical accuracy of simulation results is to perform grid refinement. The base case comprises a grid of 21×62×11. We have refined the grid by a factor of 2 both in each of the directions X and Z, individually as well as simultaneously, so that the biggest case simulated is 81×62×41. The results shown in Table 4.16 are obtained for the case of 60 and 30 laterals only. Also only the anisotropic reservoir case is refined to determine the accuracy. The following table summaries the results of grid refinement. A comparison of the PI for the base case and the refined cases indicates a good validation of the results obtained from the base case simulations. As mentioned earlier these results are obtained for an anisotropic reservoir with permeability in the three directions given as (1.0, 1.0, 0.1) md.

Table 4.16 – Results showing numerical consistency with grid refinement

Grid Structure	**Number of Laterals**	**Productivity Index, J**
A. Base Case		
21 × 62 × 11	60	26.2447
	30	13.1281
B. Grid Refinement		
Z - Direction:		
21 × 62 × 21	60	23.9285
	30	11.936
X - Direction:		
41 × 62 × 11	60	23.5568
	30	11.7413
X & Z - Direction:		
41 × 62 × 21	60	23.6054
	30	11.7428
81 × 62 × 41	60	23.429
	30	11.6357

CHAPTER V
FIELD CASE SIMULATION AND ANALYSIS

5.1 Data for El Furrial Field

El Furrial is an onshore field, located in the North of Monagas basin in Eastern Venezuela. It is conformed of three major reservoirs, Naricual Superior, Naricual Inferior and Cretaceous-01, all of them totaling approximately 6 billion barrels of oil in place. The lowest one, **Cretaceous-01 Reservoir** area is approximately 18 Km^2. Well Ful-04 discovered this reservoir in 1987 with an initial production of 4,000 BOPD 26°API oil with a ½" production choke. Figure 5.1 shows the location of the field.

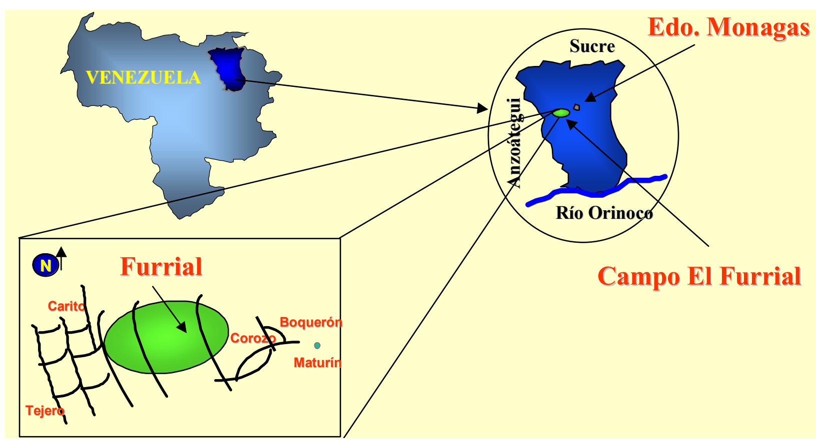

Figure 5.1 – El Furrial field location

Structural model (Figure 5.2) reveals fault-driven asymmetric anticline, NE-SW oriented. Structure is affected by several axial transversal faults. Fault throws are not greater that 500 ft. Also, NE-SW preferentially oriented normal faults where identified.

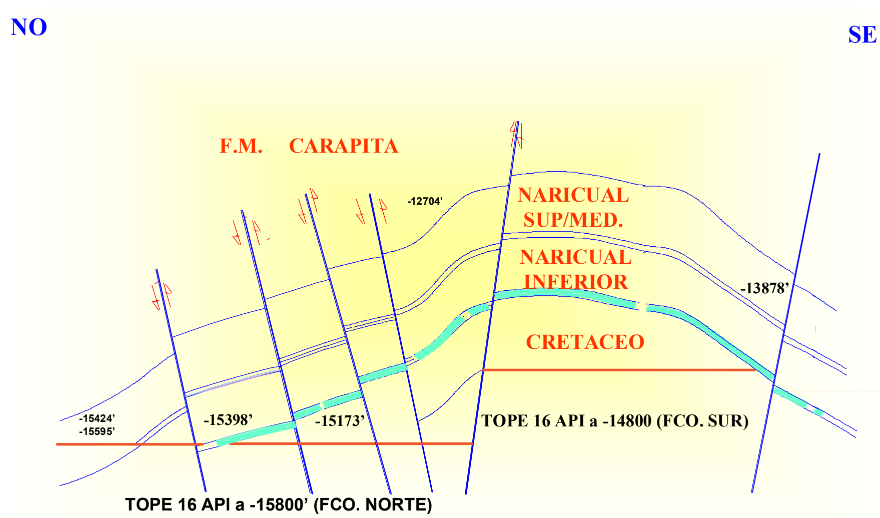

Figure 5.2 – Structural model of El Furrial

Fluid column characterization showed depth variations on thermodynamic and chemical properties, associated to gravity drainage process of the heavy components of the crude, which originated heavy crude formation and tar mat.

The main reservoir characteristics are summarized in Table 5.1

Table 5.1 – Reservoir characteristics of El Furrial

Porosity	Net ht (ft)	S_w	A	B_o (rb/stb)	μ_o (cp)	k (md)	pi(psia)
9-15%	200-800	19-24%	18 km^2	1.5	0.5-0.6	10-80	11,200

5.2 Representative Unit

To simulate the field we will consider a representation of the Cretaceous Reservoir that is simplified in many senses, but still contains the main formation characteristics and basic fluid properties. Our goal is to make the reservoir model as simple as possible, but capture all the major factors responsible for the performance differences between traditional and the suggested advanced well architecture. In the representative unit we assume x_e = 20,000 ft; y_e = 10,000 ft and h = 750 ft.

The permeability field is anisotropic. The two horizontal permeabilities are:

k_x = 86.6 md

k_y = 28.7 md

and the vertical permeability is

k_z = 2.6 md

Note the large permeability contrast between horizontal and vertical.

The porosity is 0.12, providing the oil in place. The PVT properties of the fluids are given in Table 5.2

Table 5.2 – El Furrial fluid PVT properties

P	R_s	B_o	μ
Psia	mcf/stb	rb/stb	Cp
500	0.054	1.045	7666
714	0.055	1.047	7366
1428	0.125	1.080	1251
2142	0.215	1.124	212
2857	0.335	1.185	36
3571	0.502	1.273	6
4285	0.753	1.409	1.04
4642	0.933	1.508	0.43
5000	1.172	1.640	0.17

Table 5.3 shows the variation of solution gas oil ratio with depth. It can be seen

from the data that gas volume decreases by a couple of order magnitudes within a few 1000 ft. Due to this rapid change the oil viscosity increases rapidly with depth.

Table 5.3 – Solution GOR vs. depth

Depth, ft	R_s (mcf/stb)
12000	1.145
14350	0.874
14646	0.747
14700	0.619
14800	0.538
14880	0.330
14960	0.244
15000	0.055
16500	0.055

Thus from the PVT and Solution GOR data we can see that there exist a very high contrast in mobility in the reservoir. Figure 5.3 and 5.4 shows the change in Solution GOR and Viscosity with pressure. The bar charts show the sharp change in properties with decrease in pressure. The variation of solution GOR and viscosity with depth in the reservoir is shown in Figures 5.5 and Figure 5.6 respectively.

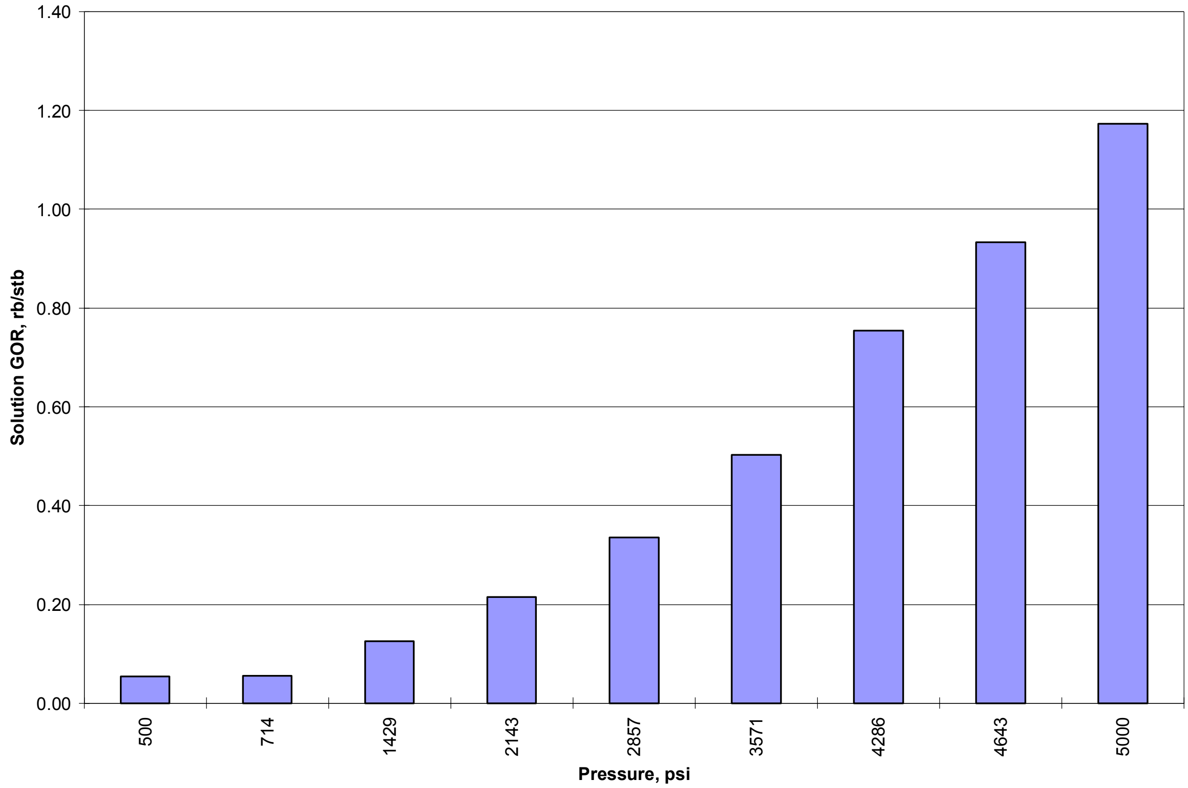

Figure 5.3– Variation of solution GOR with pressure

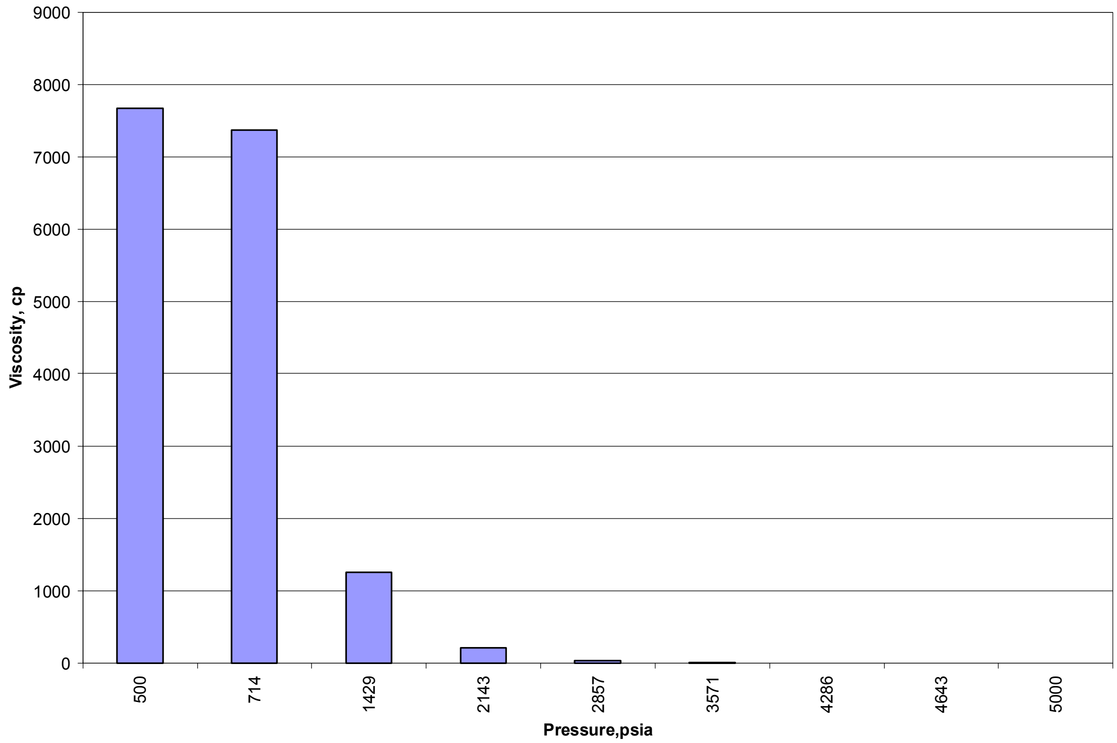

Figure 5.4– Variation of viscosity with pressure

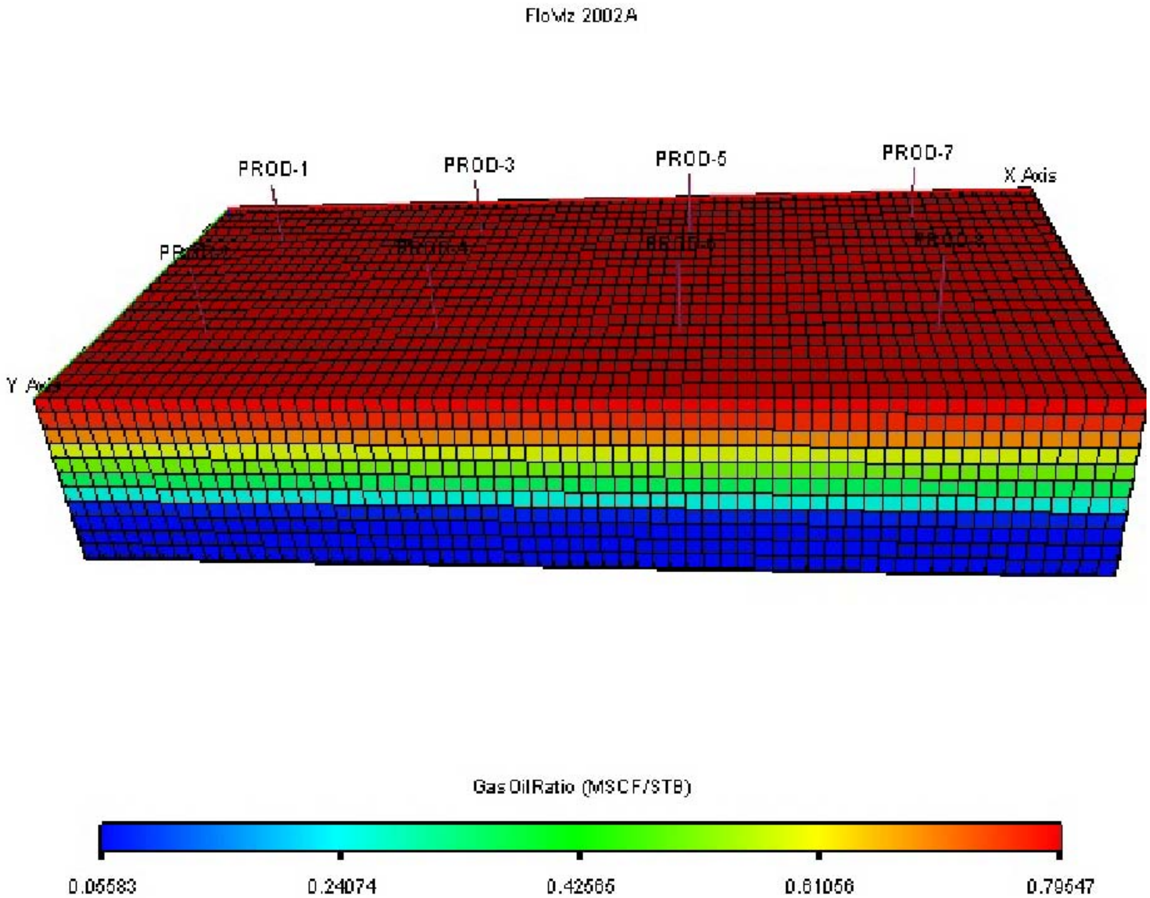

Figure 5.5– Variation of solution GOR with depth

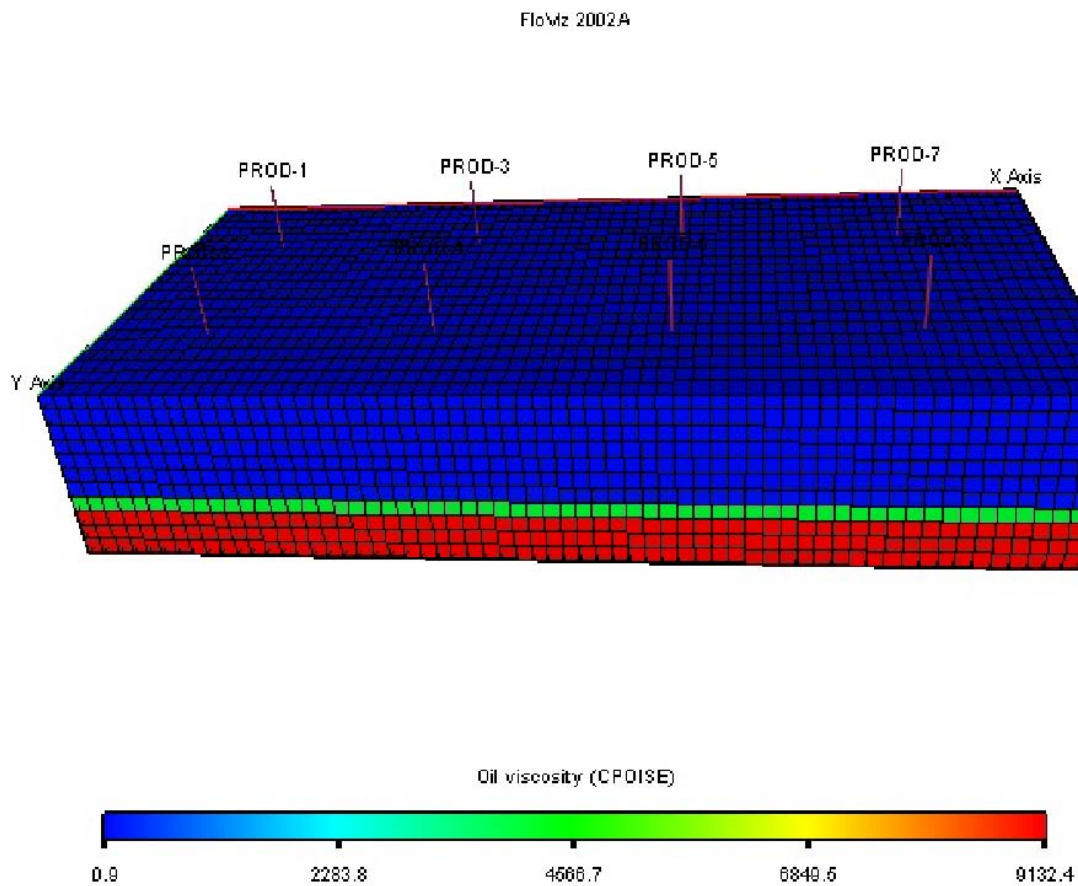

Figure 5.6 – Variation of viscosity with depth

5.3 Base Case

The basis for all comparisons is the drainage strategy of vertical wells drilled on a 1 square mile spacing basis. Hence the base case contains 8 fully penetrating vertical wells, each with equal drainage areas.

5.4 ML Well Architecture and Simulation Cases

As in all the previous ML well cases studied here too we consider the horizontal mother bore with laterals connected to drain the reservoir. However the main problem here is that of determining the location of the mother bore on account of the rapid change in properties of the fluids with depth. Hence the issue is that of optimizing the mother bore lateral in addition to determining the optimum lateral density and penetration ratio. We assume that the laterals are 100% penetrating when they extend from the mother bore to the lateral boundary. Penetration ratio (the extent of penetration) is an important design parameter to be neglected. Taking into account all of these variable the following cases have been simulated. The cases designed are described as the location of the horizontal mother bore, number of laterals and finally the penetration ratio.

Case A – Mother bore: 375 ft from top; 15 horizontal legs; Penetration: 100 %

Case B – Mother bore: 239 ft from top; 15 horizontal legs; Penetration: 100 %

Case C – Mother bore: 239 ft from top; 15 horizontal legs; Penetration: 67 %

Case D – Mother bore: 239 ft from top; 8 horizontal legs; Penetration: 100 %

Case E – Mother bore: 239 ft from top; 8 horizontal legs; penetration: 100 %

Figure 5.7 shows a general representation of the cases simulated

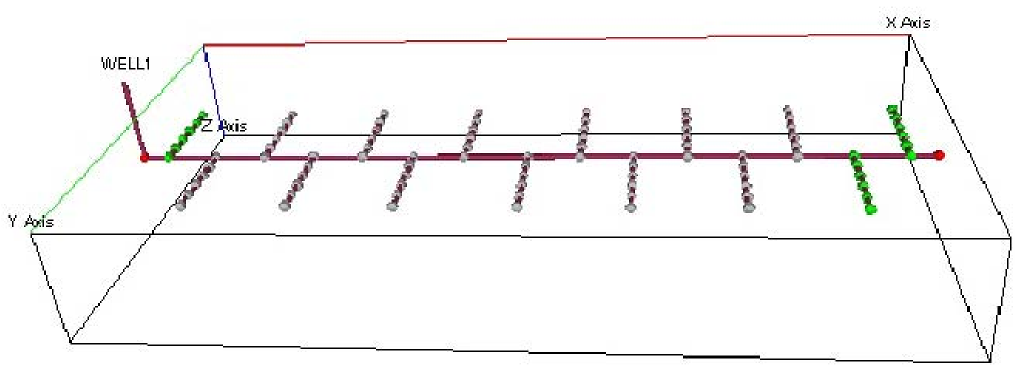

Figure 5.7 – General ML well architecture used for simulation

5.5 Simulation Results

The results of the simulation are presented in this section in Tables 5.4-5.9. The time over which the simulation is run is three years. An example input data file for the advanced well architecture case has been attached in the APPENDIX B for reference. For the economic evaluation of the technology the cumulative production is an important parameter.

Table 5.4 – Base case results (8 vertical wells)

Base Case: 8 Vertical wells							
Time	Field Pr.	W1	W1 cum	W1 bhp	ΔP	Np Cum	Gp Cum
Days	psia	stbd	MMstb	psia	psi	MMstb	Bscf
0	11,204	0	0.00	11,077	128	0.0	0.0
30	11,179	4,500	0.14	10,491	688	1.1	0.8
60	11,154	4,500	0.27	10,438	717	2.2	1.6
90	11,129	4,500	0.41	10,390	739	3.2	2.3
120	11,104	4,500	0.54	10,346	758	4.3	3.1
150	11,079	4,500	0.68	10,303	777	5.4	3.9
180	11,054	4,500	0.81	10,260	794	6.5	4.6
210	11,032	3,900	0.93	10,312	720	7.4	5.3
240	11,011	3,900	1.04	10,279	732	8.4	6.0
270	10,989	3,900	1.16	10,244	744	9.3	6.7
300	10,967	3,900	1.28	10,210	757	10.2	7.3
330	10,945	3,900	1.40	10,175	771	11.2	8.0
360	10,923	3,900	1.51	10,140	784	12.1	8.7
390	10,904	3,500	1.62	10,168	736	12.9	9.3
420	10,884	3,500	1.72	10,139	745	13.8	9.9
450	10,865	3,500	1.83	10,109	756	14.6	10.5
480	10,845	3,500	1.93	10,078	767	15.5	11.1
510	10,826	3,500	2.04	10,047	778	16.3	11.7
540	10,806	3,500	2.14	10,017	789	17.1	12.3
570	10,789	3,100	2.24	10,049	739	17.9	12.8
600	10,771	3,100	2.33	10,024	747	18.6	13.3
630	10,754	3,100	2.42	9,998	755	19.4	13.9
660	10,736	3,100	2.51	9,972	765	20.1	14.4
690	10,719	3,100	2.61	9,945	774	20.9	14.9
720	10,702	3,100	2.70	9,919	783	21.6	15.4
750	10,686	2,800	2.78	9,940	746	22.3	15.9
780	10,670	2,800	2.87	9,917	753	22.9	16.4
810	10,654	2,800	2.95	9,894	760	23.6	16.9
840	10,639	2,800	3.04	9,870	768	24.3	17.4
870	10,623	2,800	3.12	9,847	776	25.0	17.8
900	10,607	2,800	3.20	9,823	784	25.6	18.3
930	10,592	2,600	3.28	9,831	761	26.3	18.8
960	10,578	2,600	3.36	9,810	767	26.9	19.2
990	10,563	2,600	3.44	9,789	774	27.5	19.7
1020	10,549	2,600	3.52	9,767	781	28.1	20.1
1050	10,534	2,600	3.59	9,746	788	28.8	20.6
1080	10,519	2,600	3.67	9,724	795	29.4	21.0

Table 5.5 – Case A results

Case A - Motherbore 375 ft from top;15 horizontal laterals;100%							
Time	Field Pr.	W	W cum	W BHP	Δ P	Np Cum	Gp Cum
Days	psia	Stbd	MMstb	psia	psi	MMstb	Bscf
0	11,204	0	0.0	11,200	4.5	0.0	0.0
30	11,185	33,000	1.0	10,411	773.8	1.0	0.4
60	11,165	33,000	2.0	10,386	779.5	2.0	0.7
90	11,146	33,000	3.0	10,363	782.2	3.0	1.1
120	11,126	33,000	4.0	10,342	784.0	4.0	1.4
150	11,106	33,000	5.0	10,321	785.4	5.0	1.8
180	11,087	33,000	5.9	10,300	786.6	5.9	2.2
210	11,067	33,000	6.9	10,279	787.8	6.9	2.5
240	11,047	33,000	7.9	10,258	789.1	7.9	2.9
270	11,027	33,000	8.9	10,237	790.7	8.9	3.3
300	11,008	33,000	9.9	10,215	792.5	9.9	3.6
330	10,988	33,000	10.9	10,193	794.5	10.9	4.0
360	10,968	33,000	11.9	10,171	796.9	11.9	4.4
390	10,949	32,000	12.8	10,168	781.0	12.8	4.7
420	10,930	32,000	13.8	10,146	783.3	13.8	5.1
450	10,910	32,000	14.8	10,124	786.2	14.8	5.5
480	10,891	32,000	15.7	10,101	789.4	15.7	5.9
510	10,872	32,000	16.7	10,079	793.0	16.7	6.2
540	10,852	32,000	17.6	10,055	796.8	17.6	6.6
570	10,834	30,000	18.5	10,067	766.8	18.5	7.0
600	10,816	30,000	19.4	10,046	769.6	19.4	7.3
630	10,797	30,000	20.3	10,024	773.2	20.3	7.7
660	10,779	30,000	21.2	10,002	777.3	21.2	8.0
690	10,761	30,000	22.1	9,979	781.7	22.1	8.4
720	10,743	30,000	23.0	9,956	786.3	23.0	8.8
750	10,725	29,000	23.9	9,950	775.1	23.9	9.1
780	10,707	29,000	24.8	9,928	779.3	24.8	9.5
810	10,689	29,000	25.7	9,905	784.0	25.7	9.8
840	10,672	29,000	26.5	9,883	788.9	26.5	10.2
870	10,654	29,000	27.4	9,860	794.0	27.4	10.5
900	10,636	29,000	28.3	9,837	799.4	28.3	10.9
930	10,620	27,000	29.1	9,845	774.5	29.1	11.2
960	10,603	27,000	29.9	9,825	778.3	29.9	11.5
990	10,586	27,000	30.7	9,803	782.8	30.7	11.9
1020	10,570	27,000	31.5	9,782	787.7	31.5	12.2
1050	10,553	27,000	32.3	9,760	792.8	32.3	12.5
1080	10,536	27,000	33.1	9,738	798.0	33.1	12.9

Table 5.6 – Case B results

Case B - Mother bore 239 ft from top; 15 horizontal laterals;100%							
Time	Field Pr.	W	W cum	W BHP	ΔP	Np Cum	Gp Cum
Days	psia	Stbd	MMstb	psia	psia	MMstb	Bscf
0	11,204	0	0.00	11,149	55	0.00	0.00
30	11,163	63,000	1.89	10,802	360	1.89	1.11
60	11,121	63,000	3.78	10,729	392	3.78	2.23
90	11,080	63,000	5.67	10,659	421	5.67	3.35
120	11,038	63,000	7.56	10,590	448	7.56	4.47
150	10,996	63,000	9.45	10,523	474	9.45	5.60
180	10,955	63,000	11.34	10,456	499	11.30	6.73
210	10,915	60,000	13.14	10,414	501	13.10	7.80
240	10,875	60,000	14.94	10,352	523	14.90	8.88
270	10,835	60,000	16.74	10,290	545	16.70	9.96
300	10,795	60,000	18.54	10,227	568	18.50	11.00
330	10,755	60,000	20.34	10,165	590	20.30	12.10
360	10,715	60,000	22.14	10,103	612	22.10	13.20
390	10,677	57,000	23.85	10,065	612	23.90	14.20
420	10,639	57,000	25.56	10,006	632	25.60	15.30
450	10,600	57,000	27.27	9,948	653	27.30	16.30
480	10,562	57,000	28.98	9,889	673	29.00	17.30
510	10,524	57,000	30.69	9,830	694	30.70	18.40
540	10,485	57,000	32.40	9,771	714	32.40	19.40
570	10,448	55,000	34.05	9,728	721	34.10	20.40
600	10,411	55,000	35.70	9,671	740	35.70	21.40
630	10,374	55,000	37.35	9,614	759	37.40	22.40
660	10,337	55,000	39.00	9,558	779	39.00	23.40
690	10,299	55,000	40.65	9,501	798	40.70	24.40
720	10,262	55,000	42.30	9,444	818	42.30	25.40
750	10,236	38,000	43.44	9,508	728	43.40	26.10
780	10,210	38,000	44.58	9,472	738	44.60	26.80
810	10,184	38,000	45.72	9,435	749	45.70	27.50
840	10,158	38,000	46.86	9,398	760	46.90	28.20
870	10,132	38,000	48.00	9,360	772	48.00	28.90
900	10,106	38,000	49.14	9,322	784	49.10	29.60
930	10,085	30,000	50.04	9,334	752	50.00	30.20
960	10,065	30,000	50.94	9,306	759	50.90	30.70
990	10,044	30,000	51.84	9,277	768	51.80	31.30
1020	10,024	30,000	52.74	9,248	776	52.70	31.80
1050	10,003	30,000	53.64	9,218	785	53.60	32.40
1080	9,983	30,000	54.54	9,189	794	54.50	32.90

Table 5.7 – Case C results

Case C - Mother Bore 239 ft from top; 15 horizontal laterals; 67% Peneration							
Time	Field Pr.	W	W cum	W BHP	ΔP	Np Cum	Gp Cum
Days	psia	Stbd	stb	psia	psia	MMstb	Bscf
0	11,205	0	0.00	11,149	55	0.00	0.00
30	11,163	63,000	1.89	10,645	518	1.89	1.12
60	11,121	63,000	3.78	10,553	568	3.78	2.24
90	11,080	63,000	5.67	10,472	607	5.67	3.36
120	11,038	63,000	7.56	10,398	640	7.56	4.50
150	10,996	63,000	9.45	10,327	669	9.45	5.63
180	10,954	63,000	11.34	10,258	696	11.30	6.77
210	10,915	59,000	13.11	10,231	684	13.10	7.84
240	10,876	59,000	14.88	10,171	705	14.90	8.92
270	10,836	59,000	16.65	10,110	726	16.70	9.99
300	10,797	59,000	18.42	10,049	747	18.40	11.10
330	10,757	59,000	20.19	9,989	768	20.20	12.20
360	10,717	59,000	21.96	9,928	790	22.00	13.20
390	10,685	49,000	23.43	9,962	723	23.40	14.10
420	10,652	49,000	24.90	9,917	735	24.90	15.00
450	10,619	49,000	26.37	9,869	749	26.40	16.00
480	10,586	49,000	27.84	9,821	764	27.80	16.90
510	10,552	49,000	29.31	9,772	780	29.30	17.80
540	10,519	49,000	30.78	9,722	797	30.80	18.70
570	10,492	40,000	31.98	9,752	740	32.00	19.40
600	10,465	40,000	33.18	9,717	748	33.20	20.20
630	10,438	40,000	34.38	9,679	759	34.40	20.90
660	10,411	40,000	35.58	9,640	770	35.60	21.70
690	10,383	40,000	36.78	9,601	783	36.80	22.40
720	10,356	40,000	37.98	9,561	795	38.00	23.10
750	10,334	32,000	38.94	9,587	747	38.90	23.70
780	10,313	32,000	39.90	9,560	753	39.90	24.30
810	10,291	32,000	40.86	9,530	760	40.90	24.90
840	10,269	32,000	41.82	9,500	769	41.80	25.50
870	10,247	32,000	42.78	9,469	778	42.80	26.10
900	10,225	32,000	43.74	9,437	788	43.70	26.70
930	10,206	27,000	44.55	9,445	761	44.60	27.20
960	10,188	27,000	45.36	9,421	766	45.40	27.80
990	10,169	27,000	46.17	9,396	773	46.20	28.30
1020	10,151	27,000	46.98	9,371	780	47.00	28.80
1050	10,132	27,000	47.79	9,345	787	47.80	29.30
1080	10,114	27,000	48.60	9,318	795	48.60	29.80

Table 5.8 – Case D results

Case D - Mother bore 239 ft from top; 8 horizontal laterals; 100% penetration							
Time	Field Pr.	W	W cum	W BHP	ΔP	Np Cum	Gp Cum
Days	psia	Stbd	MMstb	psia	Psia	MMstb	Bscf
0	11,204	0	0.00	11,149	55	0.00	0.00
30	11,163	62,000	1.86	10,505	659	1.86	1.10
60	11,122	62,000	3.72	10,433	690	3.72	2.20
90	11,082	62,000	5.58	10,365	717	5.58	3.31
120	11,040	62,000	7.44	10,299	742	7.44	4.43
150	10,999	62,000	9.30	10,233	766	9.30	5.55
180	10,958	62,000	11.16	10,169	789	11.20	6.67
210	10,922	54,000	12.78	10,221	701	12.80	7.65
240	10,886	54,000	14.40	10,167	719	14.40	8.63
270	10,850	54,000	16.02	10,113	737	16.00	9.62
300	10,814	54,000	17.64	10,058	756	17.60	10.60
330	10,778	54,000	19.26	10,003	775	19.30	11.60
360	10,742	54,000	20.88	9,947	794	20.90	12.60
390	10,711	46,000	22.26	9,999	712	22.30	13.40
420	10,680	46,000	23.64	9,954	726	23.60	14.30
450	10,649	46,000	25.02	9,907	741	25.00	15.10
480	10,618	46,000	26.40	9,861	757	26.40	16.00
510	10,587	46,000	27.78	9,814	773	27.80	16.80
540	10,556	46,000	29.16	9,767	788	29.20	17.70
570	10,529	40,000	30.36	9,794	735	30.40	18.40
600	10,501	40,000	31.56	9,755	747	31.60	19.20
630	10,474	40,000	32.76	9,715	760	32.80	19.90
660	10,447	40,000	33.96	9,674	773	34.00	20.70
690	10,420	40,000	35.16	9,634	786	35.20	21.40
720	10,393	40,000	36.36	9,593	800	36.40	22.20
750	10,370	33,000	37.35	9,632	738	37.40	22.80
780	10,348	33,000	38.34	9,600	747	38.30	23.40
810	10,325	33,000	39.33	9,568	757	39.30	24.00
840	10,303	33,000	40.32	9,535	768	40.30	24.60
870	10,280	33,000	41.31	9,502	778	41.30	25.30
900	10,257	33,000	42.30	9,469	789	42.30	25.90
930	10,238	28,000	43.14	9,488	750	43.10	26.40
960	10,219	28,000	43.98	9,461	758	44.00	26.90
990	10,200	28,000	44.82	9,434	766	44.80	27.50
1020	10,180	28,000	45.66	9,406	774	45.70	28.00
1050	10,161	28,000	46.50	9,379	783	46.50	28.50
1080	10,142	28,000	47.34	9,351	791	47.30	29.00

Table 5.9 – Case E results

Case E - Mother bore 239 ft from top; 8 horizontal laterals; 67% penetration							
Time	Field Pr.	W	W cum	W BHP	ΔP	Np Cum	Gp Cum
Days	psia	stbd	stb	psia	Psia	stb	Mscf
0	11,204	0	0.00	11,149	55	0.00	0.00
30	11,172	49,000	1.47	10,507	665	1.47	0.87
60	11,140	49,000	2.94	10,439	700	2.94	1.75
90	11,107	49,000	4.41	10,380	727	4.41	2.63
120	11,075	49,000	5.88	10,325	749	5.88	3.52
150	11,042	49,000	7.35	10,273	769	7.35	4.41
180	11,010	49,000	8.82	10,222	787	8.82	5.30
210	10,981	43,000	10.11	10,263	718	10.10	6.09
240	10,952	43,000	11.40	10,223	729	11.40	6.88
270	10,923	43,000	12.69	10,181	742	12.70	7.68
300	10,895	43,000	13.98	10,139	755	14.00	8.47
330	10,866	43,000	15.27	10,097	769	15.30	9.27
360	10,837	43,000	16.56	10,054	783	16.60	10.08
390	10,811	38,000	17.70	10,082	729	17.70	10.79
420	10,786	38,000	18.84	10,047	738	18.80	11.50
450	10,760	38,000	19.98	10,011	749	20.00	12.21
480	10,734	38,000	21.12	9,974	761	21.10	12.92
510	10,709	38,000	22.26	9,936	772	22.30	13.64
540	10,683	38,000	23.40	9,898	785	23.40	14.35
570	10,660	34,000	24.42	9,915	745	24.40	15.00
600	10,637	34,000	25.44	9,884	753	25.40	15.64
630	10,614	34,000	26.46	9,851	763	26.50	16.28
660	10,591	34,000	27.48	9,817	773	27.50	16.93
690	10,568	34,000	28.50	9,784	784	28.50	17.57
720	10,545	34,000	29.52	9,750	795	29.50	18.22
750	10,525	29,000	30.39	9,781	744	30.40	18.77
780	10,505	29,000	31.26	9,755	750	31.30	19.33
810	10,485	29,000	32.13	9,728	757	32.10	19.88
840	10,465	29,000	33.00	9,700	765	33.00	20.43
870	10,446	29,000	33.87	9,672	774	33.90	20.99
900	10,426	29,000	34.74	9,643	783	34.70	21.54
930	10,408	26,000	35.52	9,652	756	35.50	22.04
960	10,390	26,000	36.30	9,628	762	36.30	22.54
990	10,372	26,000	37.08	9,604	769	37.10	23.04
1020	10,355	26,000	37.86	9,579	776	37.90	23.54
1050	10,337	26,000	38.64	9,553	784	38.60	24.04
1080	10,319	26,000	39.42	9,527	791	39.40	24.53

CHAPTER VI
CONCLUSIONS AND RECOMMENDATIONS

6.1 Conclusions

A new multilateral well architecture is proposed and investigated in this thesis. Its performance is compared against conventional vertical wells in most cases, as this was the original development plan used in the field. Initially parametric studies were performed to evaluate and understand performance by using simple models. These models were then applied to representative field cases and the numerical results analyzed. Also simple methods to estimate productivity are used and tested for their applicability. The following conclusions can be drawn from the study:

1. Simulations show that for the reservoir studied there exist an optimum number of laterals that can be used to drain the reservoir efficiently. Increasing the laterals after a certain number does not produce any significant difference in the cumulative production from the reservoir. For most of the cases studied 4 laterals were usually sufficient to drain the reservoir efficiently in a given period of time.

2. Parametric studies were performed by varying the lateral penetration. Initially 100% lateral penetration was assumed. However comparable production was obtained even when the penetration was lowered to 50%.

3. A comparison of results shows that to maintain a given production rate at lower branch densities much lower flowing bottom hole pressures are needed. The resulting large pressure drawdowns could cause sand production, early water or gas breakthrough or collapse of the slender laterals since they are completed open hole. To avoid such catastrophes it would be a better idea to use more laterals with lower penetration extents. This would present the added advantage of marginal reserve development while lowering drilling cost per field compared to conventional wells.

4. The numerical validation of parametric studies has been performed through a grid refinement study. The results obtained are within permissible error limits.

5. Permeability is a very important variable affecting the performance of the ML well architecture. For a given branch density the PI in the case of an isotropic permeability distribution is almost always twice the PI for anisotropic permeability variation in the reservoir. The reduced flow in the vertical direction (direction of assumed anisotropy) is the most obvious reason for this reduced productivity. However it is anticipated that better performance in anisotropic reservoirs can be achieved by using deviated laterals. Hence deviated laterals form the next direction of studies.

6. The field case studied showed that the reservoir fluid properties play a very important role in fixing the ML well architecture. The nature of the fluids is such that gas production causes the oil viscosity to rise quickly in the upper part. Hence the most desirable location of the horizontal mother bore was in the upper region of the reservoir. This essentially is indicative of the fact that a standard architecture is not necessarily effective in all cases.

7. A simple method to evaluate the maximum PI achievable using the ML well architecture is developed. Laterals have been modeled using the infinite conductivity fracture concept to arrive at this estimate which also depends upon the reservoir geometry.

8. The present analytical tool available to determine a lower limit for PI is unable to predict the performance within acceptable limits of error. The estimate is highly dependent upon the geometry and specifically the depth of the reservoir. At lower depths usually deviation between predicted and calculated values is not very large. However at large values of depth the departure between the two values is large and the calculated PI seems to attain a certain maximum value. Such

behavior is not captured by the analytical tool which does not quite account for the depth in the dimensionless PI.

6.2 Recommendations for Future Studies

The following recommendations can be made on the basis of the results and conclusions:

1. The proposed architecture is a very effective tool to better produce oil and gas. The cases analyzed were mostly homogeneous in nature.
2. The benefits of reduced cost per barrel of oil produced, greater reserve production and improved environmental footprint make it a lucrative technology which should be tested more in developing fields.
3. For heterogeneous cases a slightly modified architecture should be considered for better performance.
4. Better performance prediction tools are necessary to fully appreciate the benefits of this technology.

NOMENCLATURE

A = Drainage area (ft^2)

B = Oil formation volume factor (rb/stb)

C_A = Dietz shape factor

c_t = Compressibility factor (1/psia)

h = Reservoir depth (ft)

h_h = Reservoir height for horizontal lateral case (ft)

h_w = Completion thickness (ft)

J = Productivity Index (stbd/psia)

J_D = Dimensionless productivity index

$J_{D\max}$ = Maximum dimensionless productivity index

k = Permeability, (mD)

k_x = Permeability in the x-direction (mD)

k_y = Permeability in the y-direction (mD)

k_z = Permeability in the z-direction (mD)

p = Pressure (psia)

p_D = Dimensionless pressure

p_{res} = Average reservoir pressure (psia)

$\overline{p}_D$ = Volumetric average reservoir pressure (psia)

p_{wf} = Well bore flowing pressure (psia)

q = Flow rate (stb/d)

r = Radius (ft)

R_S = Solution GOR (rb/stb)

r_w = Well bore radius (ft)

s = Skin factor

t = Time (day)

t_D = Dimensionless time

t_{Dxf} = Dimensionless time with respect to x_f

t_{Dy_e} = Dimensionless time with respect to y_e

V = Reservoir pore volume (ft^3)

x_e = Length of rectangular reservoir in x-direction (ft)

x_f = Fracture half length (ft)

x_h = Reservoir x-dimension for horizontal lateral case (ft)

y = Length in y-direction (ft)

y_D = Dimensionless length in y-direction

y_e = Length of rectangular reservoir in y-direction (ft)

y_h = Reservoir y-dimension for horizontal lateral case (ft)

z_w = Elevation (ft)

Greek Letters

ϕ = Porosity

γ = Euler's constant, 1.78

μ = Viscosity, cp

REFERENCES

1. Oberkircher, J., Smith, R. and Thackwray, I.: "Boon or Bane? A Survey of the First 10 Years of Modern Multilateral Wells," paper SPE 84025 presented at the 2003 SPE Annual Technical Conference and Exhibition, Denver, Colorado, 5 – 8 October.

2. Oberkircher, J.: "Multilateral Technology as a Creative Reservoir Development Strategy for New and Mature Fields Alike," paper SPE 77826 presented at the 2002 SPE Asia Pacific Oil & Gas Conference and Exhibition, Melbourne, Australia, 8-10 October.

3. Vullinghs, P. and Dech, J.A.: "Multilateral Well Utilization on the Increase," paper SPE 56954 presented at the 1999 Offshore Europe Conference, Aberdeen, Scotland, 7-9 September.

4. Dittoe, S. R., Retnanto, A. and Economides, M. J.: "An Analysis of Reserves Enhancement in Petroleum Reservoirs with Horizontal and Multilateral Wells" paper SPE 37073 presented at the 1996 International Conference on Horizontal Well Technology, Calgary, Canada, 18-20 November.

5. Retnanto. A., and Economides, M.J.: "Performance of Multiple Horizontal Wells Laterals in Low-to-Medium Permeability Reservoirs," paper SPE 29647 presented at the 1995 Western Regional Meeting, Bakersfield, California, 8-10 March.

6. Oberkircher, J.: "The Economic Viability of Multilateral Wells," paper SPE 59202 presented at the 2000 IADC/SPE Drilling Conference, New Orleans, Louisiana, 23-25 February.

7. Tantawi, I., Taylor, R. and Russell, R.: "The Successful Redevelopment of Existing Well Using Multilateral Drilling Technique," paper SPE 49477 presented

at the 1998 8th International Petroleum Exhibition and Conference, Abu Dhabi, U.A.E., 11-14 October.

8. Mong, K., Al-Yami, H. and Lambe, S.: "The Application of Pressure Isolated Multilateral Junction Improves Economics in Offshore Arabian Gulf," paper SPE 77201 presented at the 2002 IADC/SPE Asia Pacific Drilling Technology, Jakarta, Indonesia, 9-11 September.

9. "Horizontal and Multilateral Wells," http://www.spe.org/spe/jsp/basic/0,,1104 _1714_1003974,00.html, 22 November 2003

10. Cavender, T., Roane, T.D. and Restarick, H.L. "Interfacing Fracturing and Sand Control Completion Strategies into Multilateral Technology; Considerations and Solutions," paper SPE 80477 presented at the 2003 SPE Asia Pacific Oil and Gas Conference and Exhibition, Jakarta, Indonesia, 15 – 17 April.

11. Berge, F., Hepburn, N., Bowling, J. and Gronas, T.: "A New Generation Multilateral System for the Troll Olje Field – Development and Case History," paper SPE 71837 presented at the 2001 Offshore Europe Conference, Aberdeen, Scotland, 4 – 7 September.

12. Rivera, N., Jensen, J.L., Spivey, J.P. and Jardon, M.: "Economic Comparisons of Multilateral and Horizontal Wells in Water-Drive Reservoirs," paper SPE 80927 presented at the 2003 SPE Production and Operations Symposium, Oklahoma City, Oklahoma, 22 – 25 March.

13. Gutierrez, O.D., Romero, A.M., Carreno, Z., Garrido, M., Leon, A. and Mohtadi, M.: "Using Multilateral Well Technology to Improve Recovery Factor by Water Flooding in a Giant Oil Field in Venezuela Lagunilla Inferior (LL-03)," paper SPE 78955 presented at the 2002 SPE International Thermal Operations and

Heavy Oil Symposium and International Horizontal Well Technology Conference, Calgary, Alberta, Canada, 4 – 7 November.

14. Redlinger, T., Constantine, J., Makin, G. Brown, C., Cooke, D. *et al*.: "Multilateral Technology Coupled with an Intelligent Completion System Provides Increased Recovery in a Mature Field at BP Wytch Farm, UK," paper SPE/IADC 79887 presented at the 2003 SPE/IADC Drilling Conference, Amsterdam, The Netherlands, 19 – 21 February.

15. Al-Azkawi, A, Taylor, G., Chadwick, R. and McGrain, B.: "Multilateral Wells Improve Development of Heavy Crude Production in the Mukhaizna Field, Sultanate of Oman," paper SPE 79021 presented at the 2002 SPE International Thermal Operations and Heavy Oil Symposium and International Horizontal Well Technology Conference, Calgary, Alberta, Canada, 4 – 7 November.

16. Larsen, L.: "Productivity Computations for Multilateral, Branched and Other Generalized and Extended Well Concepts," paper SPE 36754 presented at the 1996 SPE Annual Technical Conference and Exhibition, Denver, Colorado, 6 – 9 October.

17. Salas, J.R., Clifford, P.J. and Jenkins, D.P.: "Multilateral Well Performance Prediction," paper SPE 35711 presented at the 1996 Western Regional Meeting, Anchorage, Alaska, 22-24 May.

18. Yildiz, T.: "Long-Term Performance of Multilaterals in Commingled Reservoirs," paper SPE 78985 presented at the 2002 SPE International Thermal Operations and Heavy Oil Symposium and International Horizontal Well Technology Conference, Calgary, Alberta, Canada, 4 – 7 November.

19. Brister, R.: "Screening Variables for Multilateral Technology," paper SPE 64698 presented at the 2000 SPE International Oil and Gas Conference, Beijing, China, 7 – 10 November.

20. Holditch. S.: "The Increasing Role of Unconventional Reservoirs in the Future of Oil and Gas Business," *JPT* (November 2003) 34.

21. Valko, P.P.: "Reservoir Applications of New Multilateral Field Drainage Architectures and Related Technologies," 2002, Report No. 2, Unpublished, Texas A&M U., College Station, Texas.

22. Valko. P.P., Doublet, L.E. and Blasingame, T.A.: "Development and Application of the Multi-Well Productivity Index (MPI)," *SPEJ* (March 2000)

23. Wattenbarger, R.A., El-Banbi, A.H., Villegas, M.E. and Maggard, J.B.: "Production Analysis of Linear Flow into Fractured Tight Gas Wells," paper SPE 39931 presented at the 1998 APE Rocky Mountain Regional Low Permeability Reservoirs Symposium and Exhibition, Denver, Colorado, 5 – 8 April.

24. Economides, M.J., Hill, A.D. and Ehlig-Economides, C.: *Petroleum Production Systems*, Prentice Hall, Inc., New Jersey (1994) 25.

25. Cinco-Ley, H., Ramey, H. J. and Miller, F.G.: "Pseudo-Skin Factors for Partially Penetrating Directionally Drilled Wells," paper SPE 5589 presented at the 1975 Annual Technical Conference and Exhibition, Dallas, Texas, 28 September – 1 October.

APPENDIX A

Development of the infinite conductivity PI for the a vertical well

$$\frac{\partial^2 p}{\partial y^2} = \frac{\phi \mu c_t}{0.00633k}\frac{\partial p}{\partial t} \quad \text{(A.1)}$$

The initial and boundary conditions are given by,

Initial Condition: (Uniform Pressure Distribution)

$$p(r, t < 0) = p_i \quad \text{(A.2)}$$

Inner Boundary Condition: (Constant well rate)

$$q = \text{constant} = 0.00633\frac{\text{kA}}{\text{B}\mu}\frac{\partial p}{\partial y} \quad \text{(A.3)}$$

$$\left(\frac{\partial p}{\partial y}\right)_{y=0} = \frac{q\text{B}\mu}{0.00633\text{kA}} \quad \text{(A.4)}$$

The above condition is a direct application of Darcy's law for fluid flow in porous media.

Outer Boundary Condition: (No flow boundary)

$$\left(\frac{\partial p}{\partial y}\right)_{y=y_e} = 0 \quad \text{(A.5)}$$

Pseudo-steady state behavior is characterized by a constant pressure gradient with respect to time given by,

$$\frac{\partial p}{\partial t} = \text{constant} \quad \text{(A.6)}$$

From the definition of compressibility we get,

$$c = -\frac{1}{V}\frac{\partial V}{\partial p} \quad \text{(A.7)}$$

From eqn (3.8) we get,

$$\frac{\partial p}{\partial t} = -\frac{1}{cV}\frac{\partial V}{\partial t} \quad \text{.......... (A.8)}$$

where,

$$V = \phi A h \quad \text{.......... (A.9)}$$

Substituing eqn 3.11 into eqn. 3.10 gives,

$$\frac{\partial p}{\partial t} = -\frac{qB}{c\phi A h} \quad \text{.......... (A.10)}$$

The above equation obtained can also be used in terms of field units without applying any conversion factor.

Substituting eqn 3.12 into eqn. 3.3 gives,

$$\frac{\partial^2 p}{\partial y^2} = \frac{\phi \mu c_t}{0.00633k}\left(\frac{-qB}{c\phi A h}\right) \quad \text{.......... (A.11)}$$

The area of the rectangular geometry perpendicular to the flow is given as,

$$A = 4x_f h \quad \text{.......... (A.12)}$$

Substituting eqn 3.14 into eqn. 3.13 gives,

$$\frac{\partial^2 p}{\partial y^2} = \frac{-qB\mu}{0.00633ky_e\left(4x_f h\right)} \quad \text{.......... (A.13)}$$

In the above equation the flow rate q has units in ft^3/D which is converted to stock tank barrel units. Also we multiply divide the above equation by 2π to obtain the diffusivity equation in the form similar to the radial flow equation.

$$\frac{\partial^2 p}{\partial y^2} = -\frac{\pi}{2}\frac{141.2\, qB\mu}{khx_f y_e} \quad \text{.......... (A.14)}$$

To solve the diffusivity equation we convert it into dimensionless form using the following dimensionless groups,

$$y_D = \frac{y}{y_e} \quad \text{.......... (A.15)}$$

$$p_D = \frac{kh\left(p_i - p\right)}{141.2\, qB\mu} \quad \text{.......... (A.16)}$$

$$t_D = \frac{0.00633\, kt}{\phi \mu c_t y_e^2} \quad \text{.......... (A.17)}$$

Substituting eqns. 3.17, 3.18 and 3.19 into eqn 3.16 we obtain the dimensionless form of the diffusivity equation as,

$$\frac{\partial}{\partial y_D}\left(\frac{\partial p_D}{\partial y_D}\right)=\frac{\pi}{2}\left(\frac{y_e}{x_f}\right) \quad \text{.. (A.18)}$$

Similarly the initial and boundary conditions in terms of the dimensionless variables are given as,

Initial Condition: (Uniform Pressure Distribution)

$$p_D(r_D,t_D<0)=0 \quad \text{.. (A.19)}$$

Inner Boundary Condition: (Constant well rate)

$$\lim_{y_D\to 0}\left(\frac{\partial p}{\partial y}\right)=-\frac{\pi}{2}\left(\frac{y_e}{x_f}\right) \quad \text{.. (A.20)}$$

Outer Boundary Condition: (No flow boundary)

$$\left(\frac{\partial p}{\partial y}\right)_{y=1}=0 \quad \text{.. (A.21)}$$

Integrating eqn. 3.20 gives,

$$\left(\frac{\partial p_D}{\partial y_D}\right)=\frac{\pi}{2}\left(\frac{y_e}{x_f}\right)y_D+c_1 \quad \text{.. (A.22)}$$

Integrating the above equation once again with respect to y_D gives,

$$p_D=\frac{\pi}{2}\left(\frac{y_e}{x_f}\right)\frac{y_D^2}{2}+c_1y_D+c_2 \quad \text{.. (A.23)}$$

Apply the outer boundary condition, eqn. 3.23 to eqn. 3.25

$$c_1+\frac{\pi}{2}\left(\frac{y_e}{x_f}\right)=0 \quad \text{.. (A.24)}$$

$$\therefore c_1=-\frac{\pi}{2}\left(\frac{y_e}{x_f}\right) \quad \text{.. (A.25)}$$

Substituting eqn. 3.27 into eqn. 3.25 gives

$$p_D = \frac{\pi}{2}\left(\frac{y_e}{x_f}\right)\left(\frac{y_D^2}{2} - y_D\right) + c_2 \quad \text{(A.26)}$$

Substituting eqns. 3.14, 3.18 and 3.19 into eqn. 3.12 gives,

$$\frac{\partial p_D}{\partial t_D} = \frac{\pi}{2}\left(\frac{y_e}{x_f}\right) \quad \text{(A.27)}$$

Integrating the above equation with respect to t_D gives the average reservoir pressure as,

$$\overline{p}_D = \frac{\pi}{2}\left(\frac{y_e}{x_f}\right) t_D \quad \text{(A.28)}$$

From eqn (28) we get,

$$\overline{p}_D = \left[\frac{\pi}{2}\left(\frac{y_e}{x_f}\right)\left(\frac{y_D^3}{6} - \frac{y_D^2}{2}\right) + c_2 y_D\right]_0^1 \quad \text{(A.29)}$$

$$\therefore \overline{p}_D = \frac{\pi}{2}\left(\frac{y_e}{x_f}\right)\left(\frac{1}{6} - \frac{1}{2}\right) + c_2 \quad \text{(A.30)}$$

From eqn. 3.32 and eqn. 3.30 we get the value of c_2 as,

$$c_2 = \frac{\pi}{2}\left(\frac{y_e}{x_f}\right)\left(t_D + \frac{1}{3}\right) \quad \text{(A.31)}$$

Hence the dimensionless pressure solution for an infinite conductivity fracture is given as,

$$p_D = \frac{\pi}{2}\left(\frac{y_e}{x_f}\right)\left(\frac{y_D^2}{2} - y_D\right) + \frac{\pi}{2}\left(\frac{y_e}{x_f}\right)\left(t_D + \frac{1}{3}\right) \quad \text{(A.32)}$$

The dimensionless time variable defined in eqn. 3.19 is in terms of the reservoir length y_e. Hence the above equation can be written as,

$$p_D = \frac{\pi}{2}\left(\frac{y_e}{x_f}\right)\left(\frac{y_D^2}{2} - y_D\right) + \frac{\pi}{2}\left(\frac{y_e}{x_f}\right)\left(t_{Dy_e} + \frac{1}{3}\right) \quad \text{(A.33)}$$

But from the definition of t_D,

$$t_{Dy_e} = \frac{0.00633\, kt}{\phi \mu c_t y_e^2} = \left(\frac{x_f}{y_e}\right)^2 t_{Dx_f} \quad \text{(A.34)}$$

$$\therefore \left(\frac{y_e}{x_f}\right) t_{D y_e} = \left(\frac{x_f}{y_e}\right) t_{D x_f} \qquad \text{(A.35)}$$

Hence the general solution for the dimensionless pressure is given as,

$$p_D = \frac{\pi}{2}\left(\frac{y_e}{x_f}\right)\left(\frac{y_D^2}{2} - y_D\right) + \frac{\pi}{2}\left(\frac{x_f}{y_e}\right) t_{D x_f} + \frac{\pi}{6}\left(\frac{y_e}{x_f}\right) \qquad \text{(A.36)}$$

The solution at the well bore with $y_D = 0$ is given as,

$$p_{wD} = \frac{\pi}{2}\left(\frac{x_f}{y_e}\right) t_{D x_f} + \frac{\pi}{6}\left(\frac{y_e}{x_f}\right) \qquad \text{(A.37)}$$

The average reservoir pressure is obtained from eqn. 3.30 while the pressure at the well bore is obtained from eqn. 3.39 by substituting into the definition for dimensionless pressures and generating the corresponding pressures. These pressures are then used to obtain the PI for constant rate condition as,

$$J_{CR} = \frac{kh}{141.2\, B\mu \left[\frac{\pi}{6}\left(\frac{y_e}{x_f}\right)\right]} \qquad \text{(A.38)}$$

The general definition for PI in terms of the dimensionless PI is given as,

$$J_{CR} = \frac{kh}{141.2\, B\mu} J_D \qquad \text{(A.39)}$$

Comparing eqns. 3.40 and 3.41 we obtain the maximum dimensionless PI as,

$$J_{D,\ \max} = \frac{6}{\pi} \qquad \text{(A.40)}$$

APPENDIX B

The following data file is used to simulate a case where 15 laterals penetrate the reservoir at a depth of 365 ft from the top of the reservoir.

```
--
-- ----------------------------------------------------------------------------------------------
-- Office Simulation File - Multilateral Well Architecture is used to drain the field
-- ----------------------------------------------------------------------------------------------
--

RUNSPEC

TITLE
VERSION 1 Jabillos - 62x21x11

START
 30 'DEC' 1987 /

FIELD

GAS

OIL

WATER

DISGAS

SAVE
 'UNFORMATTED' /

MONITOR

RSSPEC

DIMENS
-- NX  NY  NZ
   62  21  11 /

WELLDIMS
-- MX   CON/WELL  GRPS  WLL/GRP
 1 671  1  1/                  -- Maximum number of connections

WSEGDIMS
 1  723  63/                   -- DIMENSION OF MULTISEGMENT WELL

-------------------------------------------------------------------------------
GRID
-------------------------------------------------------------------------------
```

```
EQUALS
-- PROP     VALUE      IX1   IX2   JY1   JY2   KZ1   KZ2

   'DX'   322.58  1          62        1          21        1          11 /
   'DY'   476.19  1          62        1          21        1          11 /
   'DZ'   68.18              1          62        1          21        1          11 /
   'TOPS'   14500            1          62        1          21        1          1  /
-- CRETACEOUS-01 RESSERVOIR , 750 FT
   'PERMX'        86.6    1          62        1          21        1     11/
   'PERMY'        28.67   1          62        1          21        1     11/
   'PERMZ'        2.6                1          62        1          21        1     11/
   'PORO'         .12                1          62        1          21        1     11/
/

GRIDFILE
2 /

INIT

--------------------------------------------------------------------------------
EDIT
--------------------------------------------------------------------------------

--------------------------------------------------------------------------------
PROPS
--------------------------------------------------------------------------------

PMAX
--          Maximum Simulation Pressure
11200 1* 1* 1*
/

DENSITY
--          Fluid Densities at Surface Conditions
--          sto          wat      gas (lbm/ft3)
        54.637      62.4       0.068432
/

ROCK
--          Rock Properties
       7000    3e-006
/

PVCO
-- Live Oil PVT Properties (Dissolved Gas)
--     pbub              Rs              Bo               vis               coil                   cvis
--    psia             mcf/stb         rb/stb            cp              1/psi                  1/psi
     500              0.054           1.045             7666          1.5296e-005         2.022e-005
     714.286          0.0558333       1.0474            7366.34       1.5296e-005         2.022e-005
     1428.57          0.125625        1.08002           1251.99       1.5296e-005         2.022e-005
     2142.86          0.215357        1.124             212.79        1.5296e-005         2.022e-005
```

```
    2857.14     0.335       1.18504    36.166     1.5296e-005    2.022e-005
    3571.43     0.5025      1.27335    6.1468     1.5296e-005    2.022e-005
    4285.71     0.75375     1.4094     1.04472    1.5296e-005    2.022e-005
    4642.86     0.933214    1.50811    0.430698   1.5296e-005    2.022e-005
    5000        1.1725      1.64093    0.177561   1.5296e-005    2.022e-005
/

PVZG
-- Dry Gas PVT Properties (using Z-factors)
-- press z-fac gas vis
-- psia          cp
--
     290
/

       500    0.922    0.03
      1000    0.922    0.03
      2000    0.893    0.03
      3000    0.902    0.03
      4000    0.935    0.03
      5000      1      0.03
/

PVTW
-- Water PVT Properties
--       p              Bw          cw             vis            cvis
--       psia           rb/stb  1/psi   cp             1/psi
     4789.7    1               3e-006        0.15     0
/

--------------------------------------------------------------------------------

STONE1
--
SWFN
--              Water Saturation Functions
--     sw         krw         pcow
       0.14       0            0
       0.16       0.00025      0
       0.2        0.00085      0
       0.3        0.0083       0
       0.4        0.035        0
       0.5        0.049        0
       0.6        0.106        0
       0.64       0.134        0
       0.7        0.19         0
       0.8        0.32         0
       0.9        0.493        0
       1          1            0
/
```

```
-- Gas rel perm and cap pressure
SGFN
--      sg      krg         pcgo
        0       0           0
        0.05    8e-006      0
        0.1     1e-005      0
        0.2     0.0025      0
        0.3     0.0133      0
        0.4     0.0434      0
        0.5     0.1082      0
        0.6     0.2285      0
        0.73    0.5107      0
        0.86    1           0
/

SOF3
-- Oil Saturation Functions
--      Soil    krow        krog
        0       0           0
        0.1     0.01        0.0001
        0.2     0.0194      0.0054
        0.3     0.028       0.009
        0.36    0.03        0.016
        0.4     0.039       0.035
        0.5     0.084       0.05
        0.6     0.173       0.1
        0.7     0.302       0.28
        0.8     0.615       0.54
        0.84    0.81        0.716
        0.86    1           1
/

-------------------------------------------------------------------------------
REGIONS
-------------------------------------------------------------------------------

-------------------------------------------------------------------------------
SOLUTION
-------------------------------------------------------------------------------

EQUIL
-- Equilibration Data Specification
14875   11200   16250    0  13000    0    1    1   -20
/

RSVD
--     depth     Rs (mcf/stb)
       12000     1.14504
       14350     0.874212
       14646     0.7475
       14700     0.619152
```

```
        14800     0.538511
        14880     0.330833
        14960     0.244157
        15000     0.0558333
        16500     0.0558333
/

-- Switch echo output off
NOECHO

DATUM
14875 /

RPTSOL
-- Initialisation Print Output
'FIP=2' 'EQUIL' 'VOIL' /

--------------------------------------------------------------------------------
SUMMARY
--------------------------------------------------------------------------------

RPTSMRY
1
/

RPTONLY

FPR

WBHP
/

FOIP

FOPR

FWPR

FGPR

FOPT

RUNSUM

EXCEL

SEPARATE
```

```
------------------------------------------------------------------------------
SCHEDULE
------------------------------------------------------------------------------

DRSDT
0.0003 1* /

RPTRST
BASIC=2 VISC /

TUNING
1* 31 8* /
11* /
4* 31 5* /

RPTSCHED
'RESTART=2' 'FIP=2' 'WELLS=4' 'CPU=1' 'TUNING' /

WSEGITER

--ITERMAX
  50  /

WELSPECS
--   NAME     GRP     I   J    BHPDTH
    WELL1  'ESTE'   1  11    14875    'OIL'  /
/

COMPDAT
--          Well   I     J   K    K      Flag .....
--          Name                  (up) (down)

WELL1    1     11        4         4         'SHUT' 2*        3.00      3*        X /
WELL1    62      11       4         4         'SHUT' 2*        3.00      3*        X /


WELL1          3        11       4        4        OPEN   2*       0.3      3*       Y        /
WELL1          3        10       4        4        OPEN   2*       0.3      3*       Y        /
WELL1          3        9        4        4        OPEN   2*       0.3      3*       Y        /
WELL1          3        8        4        4        OPEN   2*       0.3      3*       Y        /
WELL1          3        7        4        4        OPEN   2*       0.3      3*       Y        /
WELL1          3        6        4        4        OPEN   2*       0.3      3*       Y        /

WELL1          7        11       4        4        OPEN   2*       0.3      3*       Y        /
WELL1          7        12       4        4        OPEN   2*       0.3      3*       Y        /
WELL1          7        13       4        4        OPEN   2*       0.3      3*       Y        /
WELL1          7        14       4        4        OPEN   2*       0.3      3*       Y        /
WELL1          7        15       4        4        OPEN   2*       0.3      3*       Y        /
WELL1          7        16       4        4        OPEN   2*       0.3      3*       Y        /

WELL1          11       11       4        4        OPEN   2*       0.3      3*       Y        /
```

```
WELL1   11   10   4   4   OPEN   2*   0.3   3*   Y   /
WELL1   11   9    4   4   OPEN   2*   0.3   3*   Y   /
WELL1   11   8    4   4   OPEN   2*   0.3   3*   Y   /
WELL1   11   7    4   4   OPEN   2*   0.3   3*   Y   /
WELL1   11   6    4   4   OPEN   2*   0.3   3*   Y   /

WELL1   15   11   4   4   OPEN   2*   0.3   3*   Y   /
WELL1   15   12   4   4   OPEN   2*   0.3   3*   Y   /
WELL1   15   13   4   4   OPEN   2*   0.3   3*   Y   /
WELL1   15   14   4   4   OPEN   2*   0.3   3*   Y   /
WELL1   15   15   4   4   OPEN   2*   0.3   3*   Y   /
WELL1   15   16   4   4   OPEN   2*   0.3   3*   Y   /

WELL1   19   11   4   4   OPEN   2*   0.3   3*   Y   /
WELL1   19   10   4   4   OPEN   2*   0.3   3*   Y   /
WELL1   19   9    4   4   OPEN   2*   0.3   3*   Y   /
WELL1   19   8    4   4   OPEN   2*   0.3   3*   Y   /
WELL1   19   7    4   4   OPEN   2*   0.3   3*   Y   /
WELL1   19   6    4   4   OPEN   2*   0.3   3*   Y   /

WELL1   23   11   4   4   OPEN   2*   0.3   3*   Y   /
WELL1   23   12   4   4   OPEN   2*   0.3   3*   Y   /
WELL1   23   13   4   4   OPEN   2*   0.3   3*   Y   /
WELL1   23   14   4   4   OPEN   2*   0.3   3*   Y   /
WELL1   23   15   4   4   OPEN   2*   0.3   3*   Y   /
WELL1   23   16   4   4   OPEN   2*   0.3   3*   Y   /

WELL1   27   11   4   4   OPEN   2*   0.3   3*   Y   /
WELL1   27   10   4   4   OPEN   2*   0.3   3*   Y   /
WELL1   27   9    4   4   OPEN   2*   0.3   3*   Y   /
WELL1   27   8    4   4   OPEN   2*   0.3   3*   Y   /
WELL1   27   7    4   4   OPEN   2*   0.3   3*   Y   /
WELL1   27   6    4   4   OPEN   2*   0.3   3*   Y   /

WELL1   32   11   4   4   OPEN   2*   0.3   3*   Y   /
WELL1   32   12   4   4   OPEN   2*   0.3   3*   Y   /
WELL1   32   13   4   4   OPEN   2*   0.3   3*   Y   /
WELL1   32   14   4   4   OPEN   2*   0.3   3*   Y   /
WELL1   32   15   4   4   OPEN   2*   0.3   3*   Y   /
WELL1   32   16   4   4   OPEN   2*   0.3   3*   Y   /

WELL1   36   11   4   4   OPEN   2*   0.3   3*   Y   /
WELL1   36   10   4   4   OPEN   2*   0.3   3*   Y   /
WELL1   36   9    4   4   OPEN   2*   0.3   3*   Y   /
WELL1   36   8    4   4   OPEN   2*   0.3   3*   Y   /
WELL1   36   7    4   4   OPEN   2*   0.3   3*   Y   /
WELL1   36   6    4   4   OPEN   2*   0.3   3*   Y   /

WELL1   40   11   4   4   OPEN   2*   0.3   3*   Y   /
WELL1   40   12   4   4   OPEN   2*   0.3   3*   Y   /
WELL1   40   13   4   4   OPEN   2*   0.3   3*   Y   /
```

```
WELL1   40   14   4   4   OPEN   2*   0.3   3*   Y   /
WELL1   40   15   4   4   OPEN   2*   0.3   3*   Y   /
WELL1   40   16   4   4   OPEN   2*   0.3   3*   Y   /

WELL1   44   11   4   4   OPEN   2*   0.3   3*   Y   /
WELL1   44   10   4   4   OPEN   2*   0.3   3*   Y   /
WELL1   44   9    4   4   OPEN   2*   0.3   3*   Y   /
WELL1   44   8    4   4   OPEN   2*   0.3   3*   Y   /
WELL1   44   7    4   4   OPEN   2*   0.3   3*   Y   /
WELL1   44   6    4   4   OPEN   2*   0.3   3*   Y   /

WELL1   48   11   4   4   OPEN   2*   0.3   3*   Y   /
WELL1   48   12   4   4   OPEN   2*   0.3   3*   Y   /
WELL1   48   13   4   4   OPEN   2*   0.3   3*   Y   /
WELL1   48   14   4   4   OPEN   2*   0.3   3*   Y   /
WELL1   48   15   4   4   OPEN   2*   0.3   3*   Y   /
WELL1   48   16   4   4   OPEN   2*   0.3   3*   Y   /

WELL1   52   11   4   4   OPEN   2*   0.3   3*   Y   /
WELL1   52   10   4   4   OPEN   2*   0.3   3*   Y   /
WELL1   52   9    4   4   OPEN   2*   0.3   3*   Y   /
WELL1   52   8    4   4   OPEN   2*   0.3   3*   Y   /
WELL1   52   7    4   4   OPEN   2*   0.3   3*   Y   /
WELL1   52   6    4   4   OPEN   2*   0.3   3*   Y   /

WELL1   56   11   4   4   OPEN   2*   0.3   3*   Y   /
WELL1   56   12   4   4   OPEN   2*   0.3   3*   Y   /
WELL1   56   13   4   4   OPEN   2*   0.3   3*   Y   /
WELL1   56   14   4   4   OPEN   2*   0.3   3*   Y   /
WELL1   56   15   4   4   OPEN   2*   0.3   3*   Y   /
WELL1   56   16   4   4   OPEN   2*   0.3   3*   Y   /

WELL1   60   11   4   4   OPEN   2*   0.3   3*   Y   /
WELL1   60   10   4   4   OPEN   2*   0.3   3*   Y   /
WELL1   60   9    4   4   OPEN   2*   0.3   3*   Y   /
WELL1   60   8    4   4   OPEN   2*   0.3   3*   Y   /
WELL1   60   7    4   4   OPEN   2*   0.3   3*   Y   /
WELL1   60   6    4   4   OPEN   2*   0.3   3*   Y   /
/

WELSEGS
-- RECORD 1
-- Well  Depth of     Lenght Down  Vol1   Len&Dep
-- Name        Node       Tubing
  WELL1      14865          10          1*    INC  /

-- First    Last   Branch      Outlet  Lnth    Depth   Diam     Ruf-
-- Seg      Seg    Number      Seg                     Change   ness
-- Main Stem
   2      2     1        1       10       10     0.30    1.0E-3     2* /
```

```
   3      63     2        2        322.58    0       3.00    1.0E-3      2* /

64       69      3        5         476.2   0         0.3       0.001   2*        /
70       75      4        9         476.2   0         0.3       0.001   2*        /
76       81      5        13        476.2   0         0.3       0.001   2*        /
82       87      6        17        476.2   0         0.3       0.001   2*        /
88       93      7        21        476.2   0         0.3       0.001   2*        /
94       99      8        25        476.2   0         0.3       0.001   2*        /
100      105     9        29        476.2   0         0.3       0.001   2*        /
106      111     10       34        476.2   0         0.3       0.001   2*        /
112      117     11       38        476.2   0         0.3       0.001   2*        /
118      123     12       42        476.2   0         0.3       0.001   2*        /
124      129     13       46        476.2   0         0.3       0.001   2*        /
130      135     14       50        476.2   0         0.3       0.001   2*        /
136      141     15       54        476.2   0         0.3       0.001   2*        /
142      147     16       58        476.2   0         0.3       0.001   2*        /
148      153     17       62        476.2   0         0.3       0.001   2*        /
/

COMPSEGS
-- Name
  WELL1 /

-- I      J         K         Brn   Start     End          Dir    End
--                            No    Length   Length        Pent   Range

-- Main Horizontal branch
  1      11       4         2       10.00     1*      X        62  /

3        11       4         3         1*        1*       Y         6         /
7        11       4         4         1*        1*       Y         16        /
11       11       4         5         1*        1*       Y         6         /
15       11       4         6         1*        1*       Y         16        /
19       11       4         7         1*        1*       Y         6         /
23       11       4         8         1*        1*       Y         16        /
27       11       4         9         1*        1*       Y         6         /
32       11       4         10        1*        1*       Y         16        /
36       11       4         11        1*        1*       Y         6         /
40       11       4         12        1*        1*       Y         16        /
44       11       4         13        1*        1*       Y         6         /
48       11       4         14        1*        1*       Y         16        /
52       11       4         15        1*        1*       Y         6         /
56       11       4         16        1*        1*       Y         16        /
60       11       4         17        1*        1*       Y         6         /
/

WCONPROD
--  Name   Flag  Control Qoilmax            Limits  BHP
  WELL1  'OPEN'  'ORAT'      63000.00   /
/
```

```
TSTEP
6*30
/
 WCONPROD
-- Name   Flag   Control Qoilmax           Limits   BHP
  WELL1  'OPEN'  'ORAT'      59000.00   /
/

TSTEP
6*30
/

WCONPROD
--  Name   Flag  Control Qoilmax           Limits   BHP
  WELL1  'OPEN'  'ORAT'      49000.00   /
/

TSTEP
6*30
/

WCONPROD
--  Name   Flag  Control Qoilmax           Limits   BHP
  WELL1  'OPEN'  'ORAT'      40000.00   /
/

TSTEP
6*30
/

WCONPROD
--  Name   Flag  Control Qoilmax           Limits   BHP
  WELL1  'OPEN'  'ORAT'      32000.00   /
/

TSTEP
6*30
/

WCONPROD
--  Name   Flag  Control Qoilmax           Limits   BHP
  WELL1  'OPEN'  'ORAT'      27000.00   /
/

TSTEP
6*30
/

END
```

VITA

Manoj Sarfare holds a B.E. degree in petrochemical engineering from Maharashtra Institute of Technology, Pune, India. He worked with Dr. Peter Valkó as a Research Assistant on the industry funded project on Reservoir Applications of Advanced Multilateral Well Technology.

His current address: Texas A&M University

Attn.: Dr. Peter. P. Valkó

Harold Vance Department of Petroleum Engineering

3116 TAMU

College Station, TX 77843-3116

USA